

Do mixed states exhibit deep thermalisation?

Alan Sherry* and Sthitadhi Roy†

International Centre for Theoretical Sciences, Tata Institute of Fundamental Research, Bengaluru 560089, India

Deep thermalisation – where ensembles of pure states on a local subsystem, conditioned on measurement outcomes on its complement, approach universal maximum-entropy ensembles – represents a stronger form of ergodicity than conventional thermalisation. We show that this framework fails dramatically for mixed initial states, evolved unitarily, even with infinitesimal initial mixedness. To address this, we introduce a new paradigm of deep thermalisation for mixed states, fundamentally distinct from that for pure-state ensembles. In our formulation, the deep thermal ensemble arises by tracing out auxiliary degrees of freedom from a maximum-entropy ensemble defined on an augmented system, with the ensemble structure depending explicitly on the entropy of the initial state. We demonstrate that such ensembles emerge dynamically in generic, locally interacting chaotic systems. For the self-dual kicked Ising chain, which we show to be exactly solvable for a class of mixed initial states, we find exact emergence of the so-defined mixed-state deep thermal ensemble at finite times. Our results therefore lead to fundamental insights into how maximum entropy principles and deep thermalisation manifest themselves in unitary dynamics of states with finite entropy.

Understanding the out-of-equilibrium dynamics of complex quantum systems remains a central question in modern physics, bridging quantum many-body theory and quantum information science. This question has gained renewed significance with the advent of quantum computing platforms, albeit noisy, that operate far from equilibrium [1–6]. The answers to this question not only underlie the emergence of universal thermal ensembles under dynamics [7–10] but also shed light onto pertinent questions in quantum information science, such as those related to the emergence of quantum designs [11–13] and the dynamics of quantum information in general [14].

Conventional thermalisation is a statement about the emergence of thermal density matrices describing the state of local subsystems, with the rest of the system acting as a bath in the context of isolated quantum systems undergoing unitary dynamics [7–10]. Formally, the latter is equivalent to tracing out the degrees of freedom in the bath. However, modern experiments allow for microscopic interrogation of the systems by enabling measurements of non-local, multipartite correlations as well as keeping a record of the measurement outcome [15–25]. Such measurements, when restricted to the bath, induce an ensemble of states on the local subsystem conditioned on the outcomes of the measurement on the bath. The ensemble, dubbed the *projected ensemble* (PE) [25, 26], manifestly contains a lot more information than the density matrix of the subsystem as the former describes an entire distribution of states whereas the latter is just the first moment of the said distribution.

An important fallout is the extension of the ideas of thermalisation to that of *deep thermalisation* [25–35] which is the phenomenon that the PE maximises the ensemble entropy [34] which quantifies how well does the ensemble explore the available Hilbert space. In the absence of any conservation laws, the relevant ensemble is the Haar ensemble which leads to the emergence of quantum designs [25, 26]. Conservation laws modify the deep

thermal ensemble by distorting the Haar ensemble to generate the so-called Scrooge ensemble which is the maximum entropy ensemble of pure states given a density matrix as the first moment of the ensemble [29, 35–40].

The plethora of recent work on these questions have focussed almost exclusively on the pure states undergoing unitary dynamics. In this Letter, we investigate the hitherto unexplored territory of the fate of deep thermalisation when the initial state itself is mixed, or in other words, has finite entropy. This question is of fundamental interest as the nature of the induced PEs can be completely different from those in the case of pure states; in particular, the maximum entropy principle itself for ensembles of mixed states is not clearly established [41–43]. At the same time, the question is of increasingly practical importance as the presence of finite entropy due to state preparation and measurement (SPAM) errors is ubiquitous in all experimental platforms [19, 23].

In this Letter we show that deep thermalisation as defined for pure states is fragile to any amount of mixedness in the initial state even for thermodynamically large baths and maximally chaotic dynamics. Instead the asymptotic projected ensemble of mixed states is described by partially tracing out pure states from a maximum entropy ensemble, which depends on the initial state, over a system augmented by auxiliary degrees of freedom and hence defines a new paradigm for deep thermalisation of mixed states; this is shown by analytically computing arbitrary moments of the said ensembles and constitutes the first result of this work. The second key result is the demonstration of the emergence of this ensemble for locally interacting chaotic dynamics. In particular, we show analytically for an exactly solvable model that the mixed-state ensemble emerges at a finite time. We complement our exact results with numerical results away from the exactly solvable point.

To describe and explain these results concretely, let us lay out some definitions explicitly. Consider a system

bipartitioned into a subsystem A and its complement, B . The PE will be induced on the former due to measurements on the latter. Given a generic state ϱ of the system, the PE, denoted by

$$\mathcal{E}_{\text{PE}}[\varrho] := \{p(z_B), \varrho_A(z_B)\}_{z_B}, \quad (1)$$

is generated by performing projective measurements on all the degrees of freedom in B . In Eq. 1, $\varrho_A(z_B)$ is the state of A given the measurement outcome z_B ,

$$\varrho_A(z_B) = \frac{1}{p(z_B)} \text{Tr}_B[\Pi_{z_B} \varrho]; \quad p(z_B) = \text{Tr}[\Pi_{z_B} \varrho], \quad (2)$$

where $\Pi_{z_B} = |z_B\rangle\langle z_B|$ is a rank-1 projector and $p(z_B)$ is the probability of obtaining z_B as the outcome. As an example, for a system of qubits, z_B can be a bit-string $\{0, 1\}^{\otimes |B|}$ corresponding to the measurement of the Pauli- Z operator on each qubit of B . The ensemble in Eq. 1 can also be fully characterised by all its moments with the k^{th} moment given by

$$\rho_{\mathcal{E}_{\text{PE}}}^{(k)} = \sum_{z_B} p(z_B) [\varrho_A(z_B)]^{\otimes k}. \quad (3)$$

Since the PE is induced on A it is natural to consider it of finite size, $|A| \sim O(1)$, whereas the ‘measured bath’, B will be taken to be thermodynamically large, $|B| \gg 1$.

The central question of interest in this work is the fate of the PE in Eq. 1 when the corresponding ϱ is obtained from evolving an initially mixed state with a chaotic unitary circuit. We therefore need to define a reference ensemble which emerges for the PE following maximal scrambling or equivalently, by the action of an infinite-depth unitary circuit. Specifically, given an initial state ρ_0 , the reference ensemble is defined as

$$\mathcal{E}_{\text{ref}}[\rho_0] := \mathcal{E}_{\text{PE}}[U_{\text{Haar}} \rho_0 U_{\text{Haar}}^\dagger], \quad (4)$$

where U_{Haar} is a Haar-random unitary operator acting on the entire system $A \cup B$; the construction of \mathcal{E}_{ref} is depicted graphically in Fig. 1(a). The definition, 4, is guided by two rationales. First, in the limit of ρ_0 pure, $\mathcal{E}_{\text{ref}}[\rho_0]$ would necessarily deep thermalise to the Haar ensemble on A . Hence any deviation from the Haar ensemble or deep thermalisation altogether for a generic mixed ρ_0 can be attributed solely to its mixedness. Secondly, as discussed above, $U_{\text{Haar}} \rho_0 U_{\text{Haar}}^\dagger$ represents statistically a maximally scrambled state attainable from ρ_0 . Consequently, the distance of $\mathcal{E}_{\text{ref}}[\rho_0]$ from the Haar ensemble is expected to provide a bound on the distance from the Haar ensemble of the PE induced on a state resulting from evolving ρ_0 via any finite-depth unitary circuit.

With the definition of $\mathcal{E}_{\text{ref}}[\rho_0]$ firmly in place, we address the question that in what sense is it (or not) a deep thermal ensemble by computing analytically its moments defined in Eq. 3 in the limit of $|B| \rightarrow \infty$. Importantly, any moment depends solely on the eigenvalues of

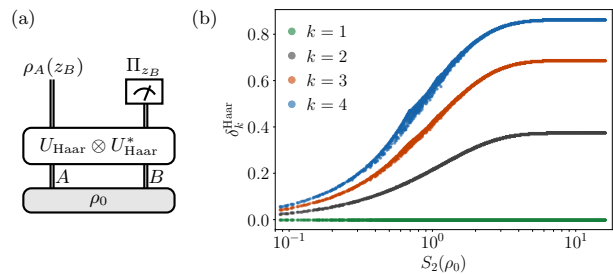


FIG. 1. (a) Schematic showing the construction of $\mathcal{E}_{\text{ref}}[\rho_0]$, defined via Eq. 4. Note that ρ_0 itself is an operator and each black line carries two sets of indices, one from the kets and other from the bras of ρ_0 . The operators U_{Haar} and U_{Haar}^\dagger acting on them, respectively, have been folded into the one white box. (b) Trace distance between the k^{th} moments of the \mathcal{E}_{mix} and the Haar ensemble plotted against the second Rényi entropy of the initial state for $|A| = 2$.

ρ_0 . While the k^{th} moment is given explicitly in Eq. 17 (End Matter) it will be sufficient to discuss $k = 1, 2$ here.

The first moment, $k = 1$, is trivially the maximally mixed state, $\rho_{\mathcal{E}_{\text{ref}}[\rho_0]}^{(k=1)} = D_A^{-1} \mathbb{I}_{D_A}$. For $k = 2$, the first non-trivial moment, it reduces to

$$\rho_{\mathcal{E}_{\text{ref}}[\rho_0]}^{(k=2)} = \frac{\mathbb{I}_{D_A^2} + (\text{Tr} \rho_0^2) \mathbb{S}_{D_A^2}}{D_A^2 + (\text{Tr} \rho_0^2) D_A}, \quad (5)$$

where $\mathbb{S}_{D_A^2}$ is the SWAP operator acting on the doubled Hilbert space $\mathcal{H}_A^{\otimes 2}$. An important corollary of the result is that the average purity of the ensemble is

$$\mathcal{P}_{\mathcal{E}_{\text{ref}}[\rho_0]} = \text{Tr} \left[\rho_{\mathcal{E}_{\text{ref}}[\rho_0]}^{(2)} \mathbb{S}_{D_A^2} \right] = \frac{1 + D_A \text{Tr} \rho_0^2}{D_A + \text{Tr} \rho_0^2} \leq 1, \quad (6)$$

with the equality appearing only for ρ_0 pure. The above inequality implies that for any finite mixedness in ρ_0 , irrespective of however small, the average purity $\mathcal{P}_{\mathcal{E}_{\text{ref}}[\rho_0]} < 1$ necessarily. Therefore, $\mathcal{E}_{\text{ref}}[\rho_0]$ cannot be described by any ensemble of pure states, which automatically rules out the Haar or a Scrooge ensemble. This leads to us to the first key result of this work – *the emergence of exact quantum designs via PEs generated from scrambling dynamics is fine-tuned to pure initial states; any finite entropy in the initial state leads to a finite departure of the PE from a design* [44]. To put this on a quantitative footing, we compute the distance of the k^{th} -moment of $\mathcal{E}_{\text{ref}}[\rho_0]$ and that of the Haar ensemble, $\delta_k^{\text{Haar}} = \|\rho_{\mathcal{E}_{\text{ref}}[\rho_0]}^{(k)} - \rho_{\text{Haar}}^{(k)}\|_1$. In Fig. 1(b), we show the results for δ_k^{Haar} as a function of the second Rényi entropy of the initial state, $S_2(\rho_0) = -\ln \text{Tr}[\rho_0^2]$ which clearly shows that the distance between $\mathcal{E}_{\text{ref}}[\rho_0]$ and the Haar ensemble grows monotonically with $S_2(\rho_0)$ for $k \geq 2$.

Having established that $\mathcal{E}_{\text{ref}}[\rho_0]$ does not correspond to any ensemble of pure states, a natural question arises that can it be described by a ‘universal’ ensemble of mixed

states. In particular, one can ask does there exist a maximum entropy ensemble of pure states on A augmented by auxiliary degrees of freedom, X , such tracing out X in the states in the ensemble yields $\mathcal{E}_{\text{ref}}[\rho_0]$. To address this question, consider a purification of ρ_0 via state $|\phi_0\rangle$ on an extended system $X \cup A \cup B$, where the dimension of X is the same as that of $A \cup B$. The state is most conveniently represented diagrammatically as,

$$|\phi_0\rangle = \left[\begin{array}{c} X \quad A \quad B \\ \sqrt{\rho_0} \\ X \quad B \end{array} \right] = \left[\begin{array}{c} X \quad A \quad B \\ \text{trapezoid} \end{array} \right], \quad (7)$$

which makes it trivial to see that $\rho_0 = \text{Tr}_X[|\phi_0\rangle\langle\phi_0|]$. Applying the Haar-random unitary on $A \cup B$ to the state $|\phi_0\rangle$ and performing measurements on B leads to a PE of pure states on $X \cup A$, $\mathcal{E}_{\text{PE}}^{XA} = \{p(z_B), |\phi_{XA}(z_B)\rangle\}_{z_B}$, where $|\phi_{XA}(z_B)\rangle$ is given by

$$|\phi_{XA}(z_B)\rangle = \left[\begin{array}{c} X \quad A \quad B \\ U_{\text{Haar}} \\ X \quad B \end{array} \right] \text{ with measurement } z_B. \quad (8)$$

$\mathcal{E}_{\text{ref}}[\rho_0]$ can be obtained from $\mathcal{E}_{\text{PE}}^{XA}$ as

$$\mathcal{E}_{\text{ref}}[\rho_0] = \{p(z_B), \text{Tr}_X |\phi_{XA}(z_B)\rangle\langle\phi_{XA}(z_B)|\}_{z_B}. \quad (9)$$

The k^{th} -moment is then given by [45]

$$\begin{aligned} \rho_{\mathcal{E}_{\text{ref}}[\rho_0]}^{(k)} &= \sum_{z_B} p(z_B) [\text{Tr}_X |\phi_{XA}(z_B)\rangle\langle\phi_{XA}(z_B)|]^{*k} \\ &= \int d\psi_{\text{Haar}} D_{XA} \frac{(\text{Tr}_X [\sqrt{\rho_{XA}} |\psi\rangle\langle\psi| \sqrt{\rho_{XA}}])^{*k}}{\langle\psi|\rho_{XA}|\psi\rangle^{k-1}}, \end{aligned} \quad (10)$$

where $d\psi_{\text{Haar}}$ is the Haar-measure over the Hilbert space of $X \cup A$ (of dimension D_{XA}) and $\rho_{XA} = (\rho_0^T \otimes \mathbb{I}_{D_A})/D_A$.

The most important fallout of the result in Eq. 10 is that it answers the question raised at the beginning of this discussion in the affirmative – *indeed $\mathcal{E}_{\text{ref}}[\rho_0]$ can be interpreted as an ensemble obtained by tracing out auxiliary degrees of freedom, X , from a maximum entropy ensemble, in this case the Scrooge ensemble, defined by the density matrix ρ_{XA} on $X \cup A$; in this sense $\mathcal{E}_{\text{ref}}[\rho_0]$ can be dubbed as a mixed state deep thermal ensemble.* A key distinction from deep thermal ensembles of pure states is that constructing $\mathcal{E}_{\text{ref}}[\rho_0]$ as a partial trace from a maximum-entropy ensemble requires the full spectrum of ρ_0 , a mixed state on a thermodynamically large system even though $\mathcal{E}_{\text{ref}}[\rho_0]$ itself is defined on a finite subsystem. In contrast, for pure states, the (finite-dimensional) density matrix of the subsystem often suffices to define the induced deep-thermal ensemble.

An interesting case of the above constructions is when all the non-zero eigenvalues of ρ_0 are the same and equal

to $1/\text{rank}(\rho_0)$. In this case, $\mathcal{E}_{\text{ref}}[\rho_0]$ is given by tracing out R from a Haar ensemble defined on $R \cup A$ [45],

$$\mathcal{E}_{\text{ref}}[\rho_0] = \{\text{Tr}_R[|\psi\rangle\langle\psi|] : |\psi\rangle \sim \text{Haar}(D_{RA})\}, \quad (11)$$

where the dimension of R is set by $D_R = \text{rank}(\rho_0)$. The ensemble in Eq. 11 is referred to as the generalised Hilbert-Schmidt ensemble (gHSe) [46–48]. The gHSe was shown [43] to emerge as the PE for lossy measurements in a fine-tuned situation with a specific choices of unitary, measurement, and initial state. Our result lays down the general conditions in which the PE is described by an appropriate gHSe.

This concludes our characterisation of $\mathcal{E}_{\text{ref}}[\rho_0]$ for ρ_0 mixed and discussion of how can it be interpreted as a deep thermal ensemble. We next discuss how $\mathcal{E}_{\text{ref}}[\rho_0]$ emerges naturally in locally interacting chaotic systems. In particular, we consider a non-integrable periodically kicked (Floquet) Ising chain for which we show numerical results and its self-dual point, we analytically prove the emergence of $\mathcal{E}_{\text{ref}}[\rho_0]$ at finite times.

For a Floquet system, the time-evolution operator for time $t \in \mathbb{Z}$ is given by $U_t = U_F^t$ with U_F the time-evolution operator over one period, often referred to as the Floquet unitary. For the kicked Ising chain,

$$U_F = U_Y U_Z = e^{-ih \sum_j Y_j} e^{-i \sum_j [J Z_j Z_{j+1} + g Z_j]}, \quad (12)$$

with $Y_j(Z_j)$ the Pauli- $Y(Z)$ operator at site j , and we consider open boundary conditions. The model can be represented as a circuit, as in Fig. 2(a) where $\blacklozenge \text{---} \blacksquare \text{---} \blacklozenge$ denotes the Ising interaction and the longitudinal fields in U_Z and $\text{---} \blacklozenge \text{---}$, the transverse kicks in U_Y . We consider initial states of the form (see Fig. 2(a))

$$\rho_0 = \rho_S \otimes \prod_{j \in E} |v_j\rangle\langle v_j|, \quad (13)$$

where ρ_S is an arbitrary mixed state on the S leftmost qubits and $|v_j\rangle$ is a random pure state of the qubit at $j \in E$ with $E = \bar{S}$. Evolution of ρ_0 with U_F for time t yields $\rho_t = U_F^t \rho_0 U_F^{\dagger t}$ from which we generate the PE, $\mathcal{E}_{\text{PE}}[\rho_t]$ on the leftmost $|A|$ qubits, by performing projective measurements on B in the computational basis. To quantify the distance between $\mathcal{E}_{\text{PE}}[\rho_t]$ and $\mathcal{E}_{\text{ref}}[\rho_0]$ with t we employ the trace distance between the k^{th} moments

$$\Delta_k(t) = \left\| \rho_{\mathcal{E}_{\text{ref}}[\rho_0]}^{(k)} - \rho_{\mathcal{E}_{\text{PE}}[\rho_t]}^{(k)} \right\|_1. \quad (14)$$

In Fig. 2(b), we show numerical results for $\Delta_k(t)$ for generic values of (J, g, h) for a few values of k ; the results show concomitantly that in the limit of $|B| \rightarrow \infty$ and $|A| \sim O(1)$, for all the considered moments, $\Delta_k(t \rightarrow \infty) \rightarrow 0$. This provides strong evidence that the moments of $\mathcal{E}_{\text{PE}}[\rho_t]$ approach those of $\mathcal{E}_{\text{ref}}[\rho_0]$ at late times. This signals the emergence of a deep thermal ensemble from a mixed initial state evolving under the kicked Ising

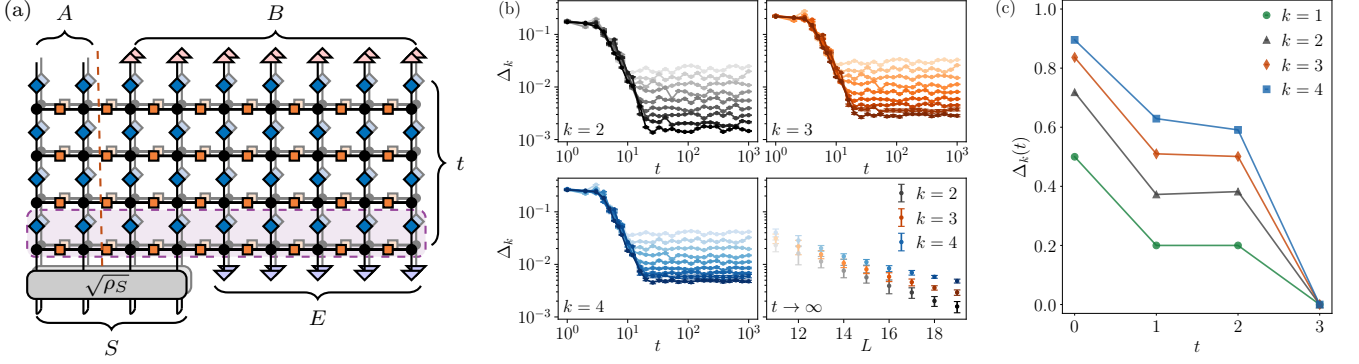


FIG. 2. (a) The kicked Ising chain in Eq. 12 as a circuit with the shaded box denoting U_F . The two copies represent U_t and U_t^\dagger . The red triangles on subsystem B denote projective measurements in the computational basis whereas the blue triangles on E along with the mixed state on S denotes the initial state in Eq. 13. (b) Results for $\Delta_k(t)$ (defined in Eq. 14) for $(J, g, h) = (0.8, 0.6472, 0.7236)$. Different panels correspond to different values of k . The initial state is of the form in Eq. 13 with $|S| = 3$. $|A| = 2$ is held fixed and different intensities correspond to different values $|B| = 9, 10, \dots, 17$ with darker colours denoting higher values. The data is averaged over 100 initial states. (c) Results for $\Delta_k(t)$ at a self-dual point $(J, g, h) = (\pi/4, \pi/9, \pi/4)$, with $|S| = 1$ and $|v_j\rangle = |+\rangle$ (see Eq. 13) in which case the moments can be computed analytically in the limit of $|B \cap E| \rightarrow \infty$.

chain, but in the limit of $t \rightarrow \infty$. The results for the timescales and finite-size scaling are relegated to Fig. 3, End Matter and the Supp. Matt. [45] respectively.

We next turn to the self-dual point of the model, $J = \pi/4 = h$, where $\text{---}\blacklozenge\text{---} = \text{---}\blacklozenge\text{---} = \text{---}\blacksquare\text{---}/\sqrt{2}$ upto an irrelevant global phase with $\text{---}\blacklozenge\text{---}$ denoting the Hadamard gate. This implies that the self-dual kicked Ising (SDKI) chain is a special instance of a dual-unitary circuit, which has enabled a range of exact results for the model (see Ref. [49] for a review and further references therein). Notably, for a pure initial state of the form $\otimes \prod_j (|+\rangle_j \langle +|)$, where $|+\rangle$ denotes an X -polarised state, evolution under the SDKI leads to the exact emergence of unitary designs: the PE coincides with the Haar ensemble exactly for $t \geq |A|$ [27]. As we discuss below, the exact solvability continues to hold for mixed initial states of the form in Eq. 13 provided $|v_j\rangle = |+\rangle \forall j \in E$.

It is useful to consider a purification of ρ_0 via a state $|\phi_0\rangle$ on an extended system $X \cup S \cup E$ where $|X| = |S|$. The SDKI unitary acting on $S \cup E$, followed by measurements on B induce a PE of pure states on $X \cup A$, $\mathcal{E}_{\text{PE}}^{XA} = \{p(z_B), \phi_{XA}(z_B)\}$, where $|\phi_{XA}(z_B)\rangle$ is given by

$$|\phi_{XA}(z_B)\rangle = \left[\begin{array}{c} X \quad A \quad \text{---}\blacklozenge\text{---} \quad z_B \\ \downarrow \quad \downarrow \quad \downarrow \\ \sqrt{\rho_S} \quad U_{\text{SDKI}}^t \quad \text{---}\blacklozenge\text{---} \\ \downarrow \quad \downarrow \quad \downarrow \\ X \quad A \quad \text{---}\blacklozenge\text{---} \quad z_{B \cap S} \\ \downarrow \quad \downarrow \quad \downarrow \\ \sqrt{\rho_S} \quad U_{\text{SDKI}}^t \quad \text{---}\blacklozenge\text{---} \\ \downarrow \quad \downarrow \quad \downarrow \\ X \quad A \quad \text{---}\blacklozenge\text{---} \quad \psi_{\text{Haar}}^{(2^t)} \end{array} \right] \quad |B \cap E| \rightarrow \infty \quad (15)$$

The statistical equivalence in the above equation implies that, in the limit of $|B \cap E| \rightarrow \infty$, for the SDKI chain with the solvable initial states, the states in $\mathcal{E}_{\text{PE}}^{XA}$ samples the ensemble of states obtained replacing the SDKI circuit acting on $B \cap E$ by a Haar random state (of dimension 2^t) in the temporal direction [27]. This crucial

simplification, which is a feature of the SDKI chain, is key towards its solvability for the class of initial mixed states discussed above. Using the standard toolbox of Haar averaging [50] and the dual-unitarity of the SDKI chain, the moments of the $\mathcal{E}_{\text{PE}}^{XA}$, comprised of states in Eq. 15, can be computed explicitly [45]. By tracing out the (copies of) X from the said moments, the moments of $\mathcal{E}_{\text{PE}}^A[\rho_0]$ can be, in turn, computed explicitly as well. For $t \geq |A| + |S|$, we find

$$\rho_{\mathcal{E}_{\text{PE}}^A[\rho_t]}^{(k)} = \int d\psi_{\text{Haar}} D_{XA} \frac{(\text{Tr}_X[\sqrt{\rho_{XA}} |\psi\rangle\langle\psi| \sqrt{\rho_{XA}}])^{\otimes k}}{\langle\psi|\rho_{XA}|\psi\rangle^{k-1}}, \quad (16)$$

where $\rho_{XA} = (\rho_S^T \otimes \mathbb{I}_{D_A})/D_A$. This is exactly analogous to Eq. 10, which demonstrates that for $t \geq |A| + |S|$, the moments of $\mathcal{E}_{\text{PE}}^A[\rho_t]$ are exactly equal to those of $\mathcal{E}_{\text{ref}}[\rho_S]$. In other words, the moments of $\mathcal{E}_{\text{PE}}^A[\rho_t]$ can be written as partial traces of the moments of a Scrooge ensemble defined on an extended system, and this emerges at a finite time $t_{\text{ref}} = |A| + |S|$. It therefore implies, that for a class of mixed initial states, dynamics with the SDKI chain does lead to the emergence of a mixed-state deep thermal ensemble on subsystem A at a finite time. While we can analytically show that Eq. 16 hold for $t \geq |A| + |S|$, our numerical results suggest that the bound is optimal and indeed $\|\rho_{\mathcal{E}_{\text{ref}}[\rho_S]}^{(k)} - \rho_{\mathcal{E}_{\text{PE}}[\rho_t=|A|+|S|]}^{(k)}\|_1 \rightarrow 0$. An exemplary result is shown in Fig. 2(c). This concludes our discussion of the kicked Ising chain. Numerical results for Floquet mixed-field Ising chain [45] also shows identical phenomenology, establishing generality.

We now close with a brief summary and some future outlook. In this work we investigated the fate of deep thermalisation under unitary dynamics of an initially mixed state, ρ_0 . We analytically compute the moments

of the PE, $\mathcal{E}_{\text{ref}}[\rho_0]$, on a state obtained by evolving ρ_0 under a generic Haar-random unitary. The results show that the notions of deep thermalisation as defined for PEs of pure states, such as emergence of quantum designs for dynamics without any conservation laws, or more generically, the emergence of maximum entropy ensembles subject to constraints placed by conservation laws are fragile to any amount of mixedness in the initial state. This implies that the phenomenology of deep thermalisation of mixed states under unitary dynamics is fundamentally different from that of pure states – this calls for a reformulation of the maximum entropy principle for mixed states. To address this, we show that $\mathcal{E}_{\text{ref}}[\rho_0]$ can be understood as a partially traced out version of a maximum entropy ensemble induced on a purification of the state on a system augmented with auxiliary degrees of freedom. The maximum entropy ensemble on the augmented system is described by a Scrooge ensemble defined by ρ_0 – this concretely defines a new paradigm for deep thermalisation of mixed states and constitutes the first main result of this work. An important conceptual point of departure from deep thermalisation for pure states is that, for mixed states the maximum entropy ensemble is defined with respect to a density matrix on a thermodynamically large system whereas for pure states the reduced density matrix of the local subsystem suffices.

While $\mathcal{E}_{\text{ref}}[\rho_0]$ is defined with reference to a Haar-random unitary, we show that it emerges robustly for generic locally interacting, chaotic dynamics. We demonstrate this numerically using a non-integrable kicked Ising chain and exploit the exact solvability (due to dual-unitarity) at its self-dual point to analytically prove the emergence of $\mathcal{E}_{\text{ref}}[\rho_0]$ at finite times. This constitutes the second main result of this work.

The general idea of deep thermalisation of mixed states is quite nascent. It is therefore natural that there several open questions of immediate interest, some of them raised by this work as well. An obvious extension of this work will be consider dynamics with conservation laws and its interplay with the extent to which ρ_0 breaks the conservation laws and to which, the measurements reveal the conserved charge. Similarly, it will be interesting to understand fate of our results in ergodicity-broken systems. In fact, our preliminary results [45] suggest that mixed-state deep thermalisation measures can serve as a sensitive probe for weak ergodicity breaking.

Within the realms of the exactly solvable SDKI chain, in our case the mixedness in the initial state was confined to a contiguous subsystem. It will be interesting to study the fate of deep thermalisation and associated timescales when the mixedness is sprinkled throughout the system. In addition, it will be interesting to develop solvable models which show distinct timescales for different moments of the PE exhibiting deep thermalisation, along the lines developed for pure states [28].

Pertinently, both decoherence and unitary scrambling

can produce featureless reduced states ($\rho_A \sim \mathbb{I}_{D_A}$) which cannot be distinguished by conventional thermalisation. However, deep-thermalisation measures, by probing higher moments can do so, and therein lies the relevance of it, especially for mixed states. Crucially, these signatures are experimentally accessible. Observables based on probabilities of probabilities (PoPs) [24] and fidelity estimators [25] provide natural probes. Our preliminary results (Fig. 4, End Matter) demonstrate that PoPs over \mathcal{E}_{ref} follow universal Erlang distributions – sharply distinct from the Porter–Thomas or δ -function statistics of pure-state designs or featureless ensembles, respectively – offering a direct operational handle on mixed-state deep thermalisation.

We thank P. W. Claeys, S. Mandal, S. Manna and G. J. Sreejith for useful discussions and collaborations on related work. This work was supported by the Department of Atomic Energy, Government of India under Project No. RTI4001, by SERB-DST, Government of India under Grant No. SRG/2023/000858 and by a Max Planck Partner Group grant between ICTS-TIFR, Bengaluru and MPIPKS, Dresden.

* alan.sherry@icts.res.in

† sthitadhi.roy@icts.res.in

- [1] J. Preskill, Quantum Computing in the NISQ era and beyond, *Quantum* **2**, 79 (2018).
- [2] S. Boixo, S. V. Isakov, V. N. Smelyanskiy, R. Babbush, N. Ding, Z. Jiang, M. J. Bremner, J. M. Martinis, and H. Neven, Characterizing quantum supremacy in near-term devices, *Nature Physics* **14**, 595–600 (2018).
- [3] A. Smith, M. Kim, F. Pollmann, and J. Knolle, Simulating quantum many-body dynamics on a current digital quantum computer, *npj Quantum Information* **5**, 106 (2019).
- [4] M. Ippoliti, K. Kechedzhi, R. Moessner, S. Sondhi, and V. Khemani, Many-body physics in the NISQ era: Quantum programming a discrete time crystal, *PRX Quantum* **2**, 030346 (2021).
- [5] J. C. Hoke, M. Ippoliti, E. Rosenberg, D. Abanin, R. Acharya, T. I. Andersen, M. Ansmann, F. Arute, K. Arya, *et al.*, Measurement-induced entanglement and teleportation on a noisy quantum processor, *Nature* **622**, 481–486 (2023).
- [6] B. Fauseweh, Quantum many-body simulations on digital quantum computers: State-of-the-art and future challenges, *Nature Communications* **15**, 2123 (2024).
- [7] J. M. Deutsch, Quantum statistical mechanics in a closed system, *Phys. Rev. A* **43**, 2046 (1991); Eigenstate thermalization hypothesis, *Rep. Prog. Phys.* **81**, 082001 (2018).
- [8] M. Srednicki, Chaos and quantum thermalization, *Phys. Rev. E* **50**, 888 (1994).
- [9] M. Rigol, V. Dunjko, and M. Olshanii, Thermalization and its mechanism for generic isolated quantum systems, *Nature* **452**, 854–858 (2008).
- [10] L. D’Alessio, Y. Kafri, A. Polkovnikov, and M. Rigol,

- From quantum chaos and eigenstate thermalization to statistical mechanics and thermodynamics, *Advances in Physics* **65**, 239–362 (2016).
- [11] D. DiVincenzo, D. Leung, and B. Terhal, Quantum data hiding, *IEEE Transactions on Information Theory* **48**, 580 (2002).
- [12] D. Gross, K. Audenaert, and J. Eisert, Evenly distributed unitaries: On the structure of unitary designs, *Journal of Mathematical Physics* **48**, 052104 (2007).
- [13] D. A. Roberts and B. Yoshida, Chaos and complexity by design, *Journal of High Energy Physics* **2017**, 1 (2017).
- [14] R. Lewis-Swan, A. Safavi-Naini, A. Kaufman, and A. Rey, Dynamics of quantum information, *Nature Reviews Physics* **1**, 627 (2019).
- [15] W. S. Bakr, J. I. Gillen, A. Peng, S. Fölling, and M. Greiner, A quantum gas microscope for detecting single atoms in a hubbard-regime optical lattice, *Nature* **462**, 74 (2009).
- [16] E. Haller, J. Hudson, A. Kelly, D. A. Cotta, B. Peaudecerf, G. D. Bruce, and S. Kuhr, Single-atom imaging of fermions in a quantum-gas microscope, *Nature Physics* **11**, 738 (2015).
- [17] C. Neill, P. Roushan, M. Fang, Y. Chen, M. Kolodrubetz, Z. Chen, A. Megrant, R. Barends, B. Campbell, B. Chiaro, *et al.*, Ergodic dynamics and thermalization in an isolated quantum system, *Nature Physics* **12**, 1037 (2016).
- [18] A. M. Kaufman, M. E. Tai, A. Lukin, M. Rispoli, R. Schittko, P. M. Preiss, and M. Greiner, Quantum thermalization through entanglement in an isolated many-body system, *Science* **353**, 794–800 (2016).
- [19] H. Bernien, S. Schwartz, A. Keesling, H. Levine, A. Omran, H. Pichler, S. Choi, A. S. Zibrov, M. Endres, M. Greiner, V. Vuletić, and M. D. Lukin, Probing many-body dynamics on a 51-atom quantum simulator, *Nature* **551**, 579 (2017).
- [20] S. Ebadi, T. T. Wang, H. Levine, A. Keesling, G. Semeghini, A. Omran, D. Bluvstein, R. Samajdar, H. Pichler, W. W. Ho, *et al.*, Quantum phases of matter on a 256-atom programmable quantum simulator, *Nature* **595**, 227 (2021).
- [21] A. Opremcak, C. H. Liu, C. Wilen, K. Okubo, B. G. Christensen, D. Sank, T. C. White, A. Vainsencher, M. Giustina, A. Megrant, *et al.*, High-fidelity measurement of a superconducting qubit using an on-chip microwave photon counter, *Phys. Rev. X* **11**, 011027 (2021).
- [22] S. J. Evered, D. Bluvstein, M. Kalinowski, S. Ebadi, T. Manovitz, H. Zhou, S. H. Li, A. A. Geim, T. T. Wang, N. Maskara, *et al.*, High-fidelity parallel entangling gates on a neutral-atom quantum computer, *Nature* **622**, 268 (2023).
- [23] S. A. Moses, C. H. Baldwin, M. S. Allman, R. Ancona, L. Ascarrunz, C. Barnes, J. Bartolotta, B. Bjork, P. Blanchard, M. Bohn, *et al.*, A race-track trapped-ion quantum processor, *Phys. Rev. X* **13**, 041052 (2023).
- [24] A. L. Shaw, D. K. Mark, J. Choi, R. Finkelstein, P. Scholl, S. Choi, and M. Endres, Experimental Signatures of Hilbert-Space Ergodicity: Universal Bitstring Distributions and Applications in Noise Learning, *Phys. Rev. X* **15**, 031001 (2025).
- [25] J. Choi, A. L. Shaw, I. S. Madjarov, X. Xie, R. Finkelstein, J. P. Covey, J. S. Cotler, D. K. Mark, H.-Y. Huang, A. Kale, H. Pichler, F. G. S. L. Brandão, S. Choi, and M. Endres, Preparing random states and benchmarking with many-body quantum chaos, *Nature* **613**, 468 (2023).
- [26] J. S. Cotler, D. K. Mark, H.-Y. Huang, F. Hernández, J. Choi, A. L. Shaw, M. Endres, and S. Choi, Emergent Quantum State Designs from Individual Many-Body Wave Functions, *PRX Quantum* **4**, 010311 (2023).
- [27] W. W. Ho and S. Choi, Exact emergent quantum state designs from quantum chaotic dynamics, *Phys. Rev. Lett.* **128**, 060601 (2022).
- [28] M. Ippoliti and W. W. Ho, Solvable model of deep thermalization with distinct design times, *Quantum* **6**, 886 (2022).
- [29] M. Lucas, L. Piroli, J. De Nardis, and A. De Luca, Generalized deep thermalization for free fermions, *Phys. Rev. A* **107**, 032215 (2023).
- [30] M. Ippoliti and W. W. Ho, Dynamical purification and the emergence of quantum state designs from the projected ensemble, *PRX Quantum* **4**, 030322 (2023).
- [31] T. Bhore, J.-Y. Desaulles, and Z. Papić, Deep thermalization in constrained quantum systems, *Phys. Rev. B* **108**, 104317 (2023).
- [32] N. D. Varikuti and S. Bandyopadhyay, Unraveling the emergence of quantum state designs in systems with symmetry, *Quantum* **8**, 1456 (2024).
- [33] A. Chan and A. De Luca, Projected state ensemble of a generic model of many-body quantum chaos, *Journal of Physics A: Mathematical and Theoretical* **57**, 405001 (2024).
- [34] D. K. Mark, F. Surace, A. Elben, A. L. Shaw, J. Choi, G. Refael, M. Endres, and S. Choi, Maximum Entropy Principle in Deep Thermalization and in Hilbert-Space Ergodicity, *Phys. Rev. X* **14**, 041051 (2024).
- [35] S. Manna, S. Roy, and G. J. Sreejith, Projected ensemble in a system with locally supported conserved charges, *Phys. Rev. B* **111**, 144302 (2025).
- [36] R. Jozsa, D. Robb, and W. K. Wootters, Lower bound for accessible information in quantum mechanics, *Phys. Rev. A* **49**, 668 (1994).
- [37] S. Goldstein, J. L. Lebowitz, R. Tumulka, and N. Zanghì, On the distribution of the wave function for systems in thermal equilibrium, *Journal of Statistical Physics* **125**, 1193 (2006).
- [38] C. Liu, Q. C. Huang, and W. W. Ho, Deep thermalization in gaussian continuous-variable quantum systems, *Phys. Rev. Lett.* **133**, 260401 (2024).
- [39] R.-A. Chang, H. Shrotriya, W. W. Ho, and M. Ippoliti, Deep thermalization under charge-conserving quantum dynamics, *PRX Quantum* **6**, 020343 (2025).
- [40] M. Bejan, B. Béri, and M. McGinley, Matchgate Circuits Deeply Thermalize, *Phys. Rev. Lett.* **135**, 020401 (2025).
- [41] A. Milekhin and S. Murciano, Observable-projected ensembles (2024), arXiv:2410.21397 [quant-ph].
- [42] A. Sherry and S. Roy, Measurement-invisible quantum correlations in scrambling dynamics, *Phys. Rev. B* **111**, L180301 (2025).
- [43] X.-H. Yu, W. W. Ho, and P. Kos, Mixed state deep thermalization (2025), arXiv:2505.07795 [quant-ph].
- [44] It can be shown that the trace distance between the k^{th} moments $\mathcal{E}_{\text{ref}}[\rho_0]$ and the Haar ensemble is bounded from below by a function $f[S_2(\rho_0)]$ which grows linearly with $S_2(\rho_0)$ for $S_2(\rho_0) \ll 1$.
- [45] See supplementary material at [URL].
- [46] M. J. Hall, Random quantum correlations and density operator distributions, *Physics Letters A* **242**, 123 (1998).
- [47] K. Życzkowski and H.-J. Sommers, Induced measures in

the space of mixed quantum states, *Journal of Physics A: Mathematical and General* **34**, 7111 (2001).

- [48] N. Bansal, W.-K. Mok, K. Bharti, D. E. Koh, and T. Haug, Pseudorandom density matrices, *PRX Quantum* **6**, 020322 (2025).
- [49] B. Bertini, P. W. Claeys, and T. Prosen, Exactly solvable many-body dynamics from space-time duality (2025), arXiv:2505.11489 [cond-mat.stat-mech].
- [50] D. Weingarten, Asymptotic behavior of group integrals in the limit of infinite rank, *Journal of Mathematical Physics* **19**, 999 (1978).
- [51] A technical point to note here is that in the limit of $|B| \rightarrow \infty$, the result in Eq. 17 holds for a single Haar-random unitary [45].
- [52] T. Brydges, A. Elben, P. Jurcevic, B. Vermersch, C. Maier, B. P. Lanyon, P. Zoller, R. Blatt, and C. F. Roos, Probing rényi entanglement entropy via randomized measurements, *Science* **364**, 260 (2019), <https://www.science.org/doi/pdf/10.1126/science.aau4963>.
- [53] M. Ledoux, The concentration of measure phenomenon, *AMS Surveys and Monographs* **89** (2001).

END MATTER

Moments of \mathcal{E}_{ref}

In the main text, we mentioned that the k^{th} moment of $\mathcal{E}_{\text{ref}}[\rho_0]$ depends only on the eigenvalues of ρ_0 . It is given explicitly as [51],

$$\rho_{\mathcal{E}_{\text{ref}}[\rho_0]}^{(k)} = \frac{\sum_{\sigma \in \mathcal{S}_k} h_{\sigma}(\rho_0) \text{Perm}_{\mathcal{H}_A^{\otimes k}}(\sigma)}{\sum_{\sigma \in \mathcal{S}_k} h_{\sigma}(\rho_0) D_A^{|\sigma|}}, \quad (17)$$

where $\text{Perm}_{\mathcal{H}_A^{\otimes k}}(\sigma)$ permutes the k copies of the D_A -dimensional Hilbert space of A , \mathcal{H}_A , according to an element σ in the permutation group of k elements \mathcal{S}_k . The dependence of the moment on ρ_0 via its eigenvalues is in $h_{\sigma}(\rho_0) \in [0, 1]$, given by

$$h_{\sigma}(\rho_0) = \text{Tr} \rho_0^{n_1} \dots \text{Tr} \rho_0^{n_{|\sigma|}} = \sum_{l_1 \dots l_{|\sigma|}} \lambda_{l_1}^{n_1} \dots \lambda_{l_{|\sigma|}}^{n_{|\sigma|}}, \quad (18)$$

where $|\sigma|$ is the number of cycles and n_m is the order of the m^{th} cycle of σ with $\sum_{m=1}^{|\sigma|} n_m = k$. Here $\{\lambda_i\}$ denotes the set of eigenvalues of ρ_0 .

While the derivations of Eq. 17 and Eq. 18 are relegated to the Supp. Matt. [45], we discuss some pertinent cases here. Two trivial limits are (i) ρ_0 pure where $h_{\sigma}(\rho_0) = 1 \forall \sigma$ in which case $\mathcal{E}_{\text{ref}}[\rho_0]$ reduces to the Haar ensemble as expected [26], and (ii) $\rho_0 \propto \mathbb{I}$; in this case $h_{\sigma}(\rho_0) = \delta_{e\sigma}$ where σ is the identify element of \mathcal{S}_k where moments of $\mathcal{E}_{\text{ref}}[\rho_0]$ are trivially $\propto \mathbb{I}^{\otimes k}$.

Mixed-state deep-thermalisation timescales

In the main text, we demonstrated for the kicked Ising chain that in the limit $|B| \rightarrow \infty$, the projected ensemble approaches $\mathcal{E}_{\text{ref}}[\rho_0]$, with $\Delta_k \rightarrow 0$ as $t \rightarrow \infty$. It

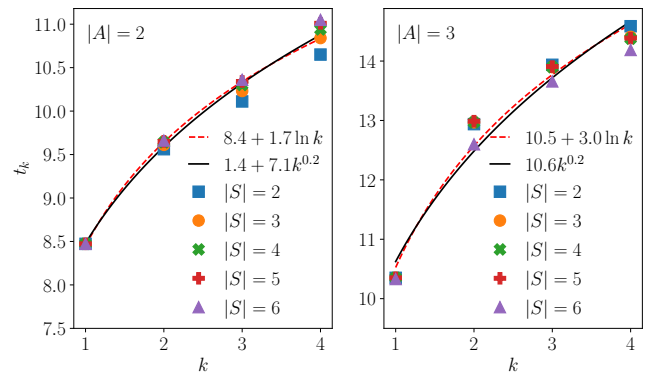


FIG. 3. Estimated behaviour of the deep-thermalisation timescale t_k with k for the kicked Ising chain. The data show no dependence of t_k on $|S|$ and a slow increase with k , consistent with both logarithmic and sub-linear power-law growth. The timescale t_k was estimated by setting a threshold $\epsilon = 3 \times 10^{-2}$ and identifying the time at which Δ_k drops below ϵ .

is therefore natural to ask what hierarchy of timescales emerges as a function of k and $|S|$. Using finite-size scaling analyses (details are provided in the Supplementary Material [45]), we first establish that in the limit $|B| \rightarrow \infty$, the dynamical behaviour of $\Delta_k(t)$ with t is independent of $|S|$. This implies that the mixed-state deep-thermalisation timescales are independent of subsystem size $|S|$. To extract the dependence of the timescales on k , as is customary (see, for example, Ref. [26]), we set a fixed threshold ϵ and determine the timescale t_k at which $\Delta_k(t)$ drops below ϵ .

The behaviour of the resulting timescale t_k is shown in Fig. 3. As expected, we find no systematic dependence of t_k on $|S|$. By contrast, t_k exhibits a slow growth with k . Our results are consistent with both a logarithmic scaling $t_k \sim \ln k$ and a sublinear power-law scaling $t_k \sim k^{0.2}$; however, within the limits of our numerics, we cannot unambiguously distinguish between the two. We note that a logarithmic dependence $t_k \sim \ln k$ is consistent with the scaling of design times observed in other toy models of deep thermalisation [28, 43].

Probabilities of (bitstring) probabilities

As an experimental and operational probe of mixed-state deep thermalisation we present some results for the probabilities of (bitstring) probabilities (PoPs) over the projected ensemble. Formally, they are defined over the PE in Eq. 1, for a bit string z_A , as

$$\text{PoP}_{z_A}(\tilde{p}) = \sum_{z_B} p(z_B) \delta(\tilde{p} - \tilde{p}(z_A|z_B)), \quad (19)$$

where $p(z_A|z_B) = \text{Tr}[\rho_A] \langle z_A | \rho_A(z_B) \rangle$ is the probability of obtaining the bitstring z_A in the conditional

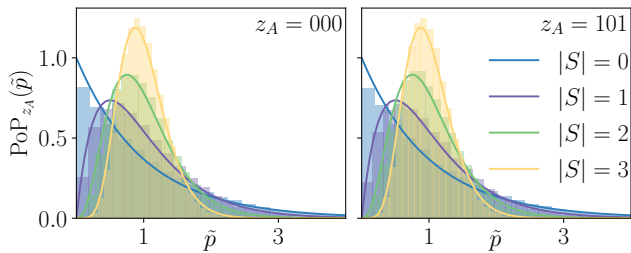


FIG. 4. The PoPs over the projected ensemble for the kicked Ising chain at a late time of $t = 1000$ for $L = 19$ and $|A| = 3$. Different colours correspond to different $|S| = 0, 1, 2, 3$ (which also tunes the entropy of the initial state). The histograms correspond to the numerical data whereas the solid lines denote the Erlang distribution (Eq. 20) for the corresponding D_S . The two panels denote two different bitstrings in A .

state $\varrho_A(z_B)$ and the $\tilde{p}(z_A|z_B) = p(z_A|z_B)/\langle p(z_A) \rangle$ denotes the relative probability with $\langle p(z_A) \rangle = \sum_{z_B} p(z_B)p(z_A|z_B)$.

The results are shown for the kicked Ising chain at a late time of $t = 10^3$, for two representative bitstrings $z_A = 000$ and $z_A = 101$, in Fig. 4. The results are for the case when ρ_S in the initial state in Eq. 13 was chosen to be maximally mixed.

Remarkably, the PoPs for any non-zero $|S|$ are extremely well described by the Erlang distribution, $P_{\text{Erlang}}(\tilde{p}; D_S)$, given by,

$$P_{\text{Erlang}}(\tilde{p}; D_S) = \frac{D_S^{D_S}}{(D_S - 1)!} e^{-D_S \tilde{p}} \tilde{p}^{D_S - 1}. \quad (20)$$

For $|S| = 0$ (equivalently $D_S = 1$), the distribution above reduces to the Porter-Thomas distribution characteristic of pure-state designs. More importantly, this Erlang distribution can experimentally signify the non-trivial moments of the projected ensemble and distinguish it from a trivial ensemble. For the latter (say, due to decoherence), $\varrho_A(z_B) \sim \mathbb{I}_{D_A}$ which would lead to $\text{PoP}_{z_A}(\tilde{p}) = \delta(\tilde{p} - 1)$.

The emergence of the Erlang distribution for mixed-state deep thermalisation can be understood straightforwardly as the projected ensemble approaches a gHSe at late times. The gHSe is nothing but a partial trace of the Haar ensemble with the PoPs in the latter described by a Porter-Thomas distribution. The bitstring probabilities in the gHSe are then simply sums of D_S Porter-Thomas distributed variables, which are distributed according to the Erlang distribution in Eq. 20.

Determining second-order Rényi entropies without randomised measurements

As a practical application of mixed-state deep thermalisation, here we demonstrate a new method to estimate the second-order Rényi entropy of an arbitrary many-body mixed state. The method relies on the fact that

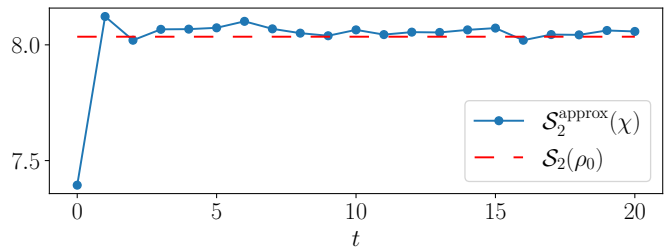


FIG. 5. The proxy for the second Rényi entropy from the bitstring probabilities (solid line) plotted against time for the kicked Ising model for $L = 12$ and $|A| = 3$. The dashed line denotes the theoretical value of the second Rényi entropy of the initial state ρ_0 which is a random mixed state with its eigenvalues sampled from a uniform Dirichlet distribution and its eigenvectors sampled from the Haar measure on $U(2^L)$.

the bitstring PoPs at late times, which are experimentally accessible, encode information about the spectrum of the initial mixed state. The method is analogous to the randomised measurement protocol [52], where local random unitaries sampled from a 2-design are applied on a mixed state, and the purity is estimated from the unitary-averaged cross-correlations of bitstring probabilities. By contrast, our method does not require any averaging over unitaries and is useful in practical settings where one is unable to sample sufficiently random ensembles of unitaries.

For instance, consider the evolution of a mixed state ρ_0 by the kicked Ising chain. To estimate the second Rényi entropy of ρ_0 , we define the correlator χ given by

$$\chi = \sum_{z_A, z_B} p(z_A, z_B) p(z_A/z_B), \quad (21)$$

where $p(z_A, z_B)$ and $p(z_A/z_B)$ are the joint and conditional bitstring probabilities, respectively. The proxy for the second Rényi entropy $\mathcal{S}_2(\rho_0)$ is defined by

$$\mathcal{S}_2^{\text{approx}}(\chi) = -\ln \left[\frac{D_A - 1}{1 - \chi} - D_A \right]. \quad (22)$$

Since the second moment of the mixed-state projected ensemble is approximately equal to that of $\mathcal{E}_{\text{ref}}[\rho_0]$ after evolving the state for sufficiently long times, we have

$$\mathcal{S}_2(\rho_0) \approx \mathcal{S}_2^{\text{approx}}(\chi), \quad (23)$$

which follows from Eq. 5 of the main text. To verify Eq. 23, we consider the kicked Ising evolution of an arbitrary mixed state ρ_0 over 12 qubits. In Fig. 5, we see that $\mathcal{S}_2^{\text{approx}}(\chi)$ converges rapidly to $\mathcal{S}_2(\rho_0)$, demonstrating the utility of mixed state deep thermalisation in learning the finer features of quantum states.

Supplementary Material: Do mixed states exhibit deep thermalisation?

Alan Sherry and Sthitadhi Roy

International Centre for Theoretical Sciences, Tata Institute of Fundamental Research, Bengaluru 560089, India

The supplementary material consists of eight sections. Sec. I is devoted to the details of the analytic computation of the moments of $\mathcal{E}_{\text{ref}}[\rho_0]$, followed by a discussion on the typicality of $\mathcal{E}_{\text{ref}}[\rho_0]$ over the Haar ensemble in Sec. II. In Sec. III, we prove the relation between $\mathcal{E}_{\text{ref}}[\rho_0]$ and the appropriate Scrooge ensemble. In Sec. IV, we detail the conditions under which the $\mathcal{E}_{\text{ref}}[\rho_0]$ reduces to the appropriate generalised Hilbert-Schmidt ensemble. The finite-size scaling analyses of $\Delta_k(t)$ and the details of extraction of the deep-thermalisation timescale for the kicked Ising chain are presented in Sec. V. In Sec. VI, we prove the emergence of $\mathcal{E}_{\text{ref}}[\rho_0]$ in finite time in the self-dual kicked Ising model. In Sec. VII we present results for the Floquet mixed-field Ising chain with the measurements in a non-computational basis whereas Sec. VIII is dedicated to the results for the PXP model to understand the fate of mixed-state deep thermalisation in weak ergodicity breaking systems

I. COMPUTATION OF THE MOMENTS OF $\mathcal{E}_{\text{ref}}[\rho_0]$

In this section, we derive Eq. 17 and Eq. 18 of the End Matter. Given the initial state ρ_0 (of a d -dimensional Hilbert space), the unitarily evolved states are of the form $U\rho_0U^\dagger$, where $U \sim \text{Haar}(d)$. The projected ensemble $\mathcal{E}_{\text{ref}}[\rho_0] := \{p(z_B), \rho_A(z_B)\}$ is generated by applying on ρ a set of rank-1 projection operators $\{|z\rangle\langle z|_B\}$. Consider the spectral decomposition of ρ_0 ,

$$\rho_0 = \sum_l \lambda_l |l\rangle\langle l|.$$

where $\lambda_l \in [0, 1]$ with $\sum_l \lambda_l = 1$. For notational convenience, we define

$$|\tilde{\chi}_{z,l}(U)\rangle := (I_A \otimes \langle z|_B) U |l\rangle, \quad (\text{S1})$$

which enables us to define

$$\begin{aligned} \mathcal{R}_z(U) &:= \sum_l \lambda_l |\tilde{\chi}_{z,l}(U)\rangle\langle \tilde{\chi}_{z,l}(U)|. \\ \mathcal{P}_z(U) &:= \text{Tr}[\mathcal{R}_z(U)], \end{aligned} \quad (\text{S2})$$

such that $p(z_B) = \mathcal{P}_z(U)$ and $\rho_A(z_B) = \mathcal{R}_z(U)/\mathcal{P}_z(U)$. Consider the unitary $U_A \in \mathcal{H}_A$, where \mathcal{H}_A is the d_A -dimensional Hilbert space over A . Let $\tilde{U} := U_A \otimes I_B$. We then have,

$$\begin{aligned} \mathcal{R}_z(\tilde{U}U) &= U_A \mathcal{R}_z(U) U_A^\dagger, \\ \mathcal{P}_z(\tilde{U}U) &= \mathcal{P}_z(U). \end{aligned} \quad (\text{S3})$$

For $U_A \sim \text{Haar}(d_A)$ and $U \sim \text{Haar}(d)$, $\mathcal{R}_z(\tilde{U}U)$ is equivalent to $\mathcal{R}_z(U)$ in a statistical sense. To compute the moments $\rho_{\mathcal{E}_{\text{ref}}[\rho_0]}^{(k)}$, we have

$$\rho_{\mathcal{E}_{\text{ref}}[\rho_0]}^{(k)} = \sum_{z_B} p(z_B) \rho_A(z_B)^{\otimes k} = \sum_z \frac{(\mathcal{R}_z(U))^{\otimes k}}{\mathcal{P}_z(U)^{k-1}}. \quad (\text{S4})$$

We derive the moments of the ensembles by averaging over $U \sim \text{Haar}(d)$. With appropriate concentration inequalities derived from Levy's lemma, it can be shown that a single random unitary can yield this ensemble (see Sec. II). Using

the statistical equivalence of $\mathcal{R}_z(\tilde{U}U)$ and $\mathcal{R}_z(U)$, we have

$$\begin{aligned}
\mathbb{E}_{U \sim \text{Haar}(d)} \left[\frac{(\mathcal{R}_z(U))^{\otimes k}}{\mathcal{P}_z(U)^{k-1}} \right] &= \mathbb{E}_{U \sim \text{Haar}(d)} \mathbb{E}_{U_A \sim \text{Haar}(d_A)} \left[\frac{(\mathcal{R}_z(\tilde{U}U))^{\otimes k}}{\mathcal{P}_z(\tilde{U}U)^{k-1}} \right] \\
&= \mathbb{E}_{U \sim \text{Haar}(d)} \mathbb{E}_{U_A \sim \text{Haar}(d_A)} \left[\frac{(U_A \mathcal{R}_z(U) U_A^\dagger)^{\otimes k}}{\mathcal{P}_z(U)^{k-1}} \right] \\
&= \mathbb{E}_{U \sim \text{Haar}(d)} \left[\frac{1}{\mathcal{P}_z(U)^{k-1}} \right] \sum_{l_1 \dots l_k} \lambda_{l_1} \dots \lambda_{l_k} \times \\
&\quad \mathbb{E}_{V \sim \text{Haar}(d)} [|\tilde{\chi}_{z,l_1}^A(V)\rangle \langle \tilde{\chi}_{z,l_1}^A(V)| \otimes \dots \otimes |\tilde{\chi}_{z,l_k}^A(V)\rangle \langle \tilde{\chi}_{z,l_k}^A(V)|] ,
\end{aligned} \tag{S5}$$

To pass from the second line to the third, we used the fact that $U_A |\tilde{\chi}_{z,l}(U)\rangle \langle \tilde{\chi}_{z,l}(U)| U_A^\dagger$ is independent of U in the limit $|B| \rightarrow \infty$ (see the independence argument in the latter part of this section for a rigorous justification) and that $U_A |\tilde{\chi}_{z,l}(U)\rangle$ is identically distributed to $|\tilde{\chi}_{z,l}^A(V)\rangle$, where $V \sim \text{Haar}(d)$.

We need not explicitly compute the Haar integral $\mathbb{E}_{U \sim \text{Haar}(d)} \left[\frac{1}{\mathcal{P}_z(U)^{k-1}} \right]$ (and doing so would require further approximations). Rather we absorb all factors in the normalisation \mathcal{N} , which is constrained by the fact that the trace of the above tensor is $\mathbb{E}_{U \sim \text{Haar}(d)} \mathcal{P}_z(U)$. This leaves us with

$$\rho_{\mathcal{E}_{\text{ref}}[\rho_0]}^{(k)} = \mathcal{N} \sum_{l_1 \dots l_k} \lambda_{l_1} \dots \lambda_{l_k} \mathbb{E}_{V \sim \text{Haar}(d)} [|\tilde{\chi}_{z,l_1}^A(V)\rangle \langle \tilde{\chi}_{z,l_1}^A(V)| \otimes \dots \otimes |\tilde{\chi}_{z,l_k}^A(V)\rangle \langle \tilde{\chi}_{z,l_k}^A(V)|] . \tag{S6}$$

The right part of the above term can be easily evaluated using Weingarten calculus, yielding the result that the projected ensemble is a non-universal ensemble that is a highly non-trivial function of the the eigenvalues of the initial mixed state. The Haar-averaged tensor in Eq. S4 can now be represented as

$$\rho_{\mathcal{E}_{\text{ref}}[\rho_0]}^{(k)} = \mathcal{N} \sum_{\sigma, \tau \in S_k} \sum_{l_1 \dots l_{|\tau|}} \lambda_{l_1}^{n_1} \dots \lambda_{l_{|\tau|}}^{n_{|\tau|}} \text{Wg}(\sigma \tau^{-1}, d) \text{Perm}_{\mathcal{H}_A^{\otimes k}}(\sigma) , \tag{S7}$$

where $|\tau|$ is the number of cycles and n_m is the order of the m^{th} cycle of τ with $\sum_{m=1}^{|\tau|} n_m = k$. Since $d \rightarrow \infty$, we have $\text{Wg}(\sigma \tau^{-1}, d) \sim \delta_{\sigma, \tau}$, which gives

$$\rho_{\mathcal{E}_{\text{ref}}[\rho_0]}^{(k)} = \mathcal{N} \sum_{\sigma \in S_k} \sum_{l_1 \dots l_{|\sigma|}} \lambda_{l_1}^{n_1} \dots \lambda_{l_{|\sigma|}}^{n_{|\sigma|}} \text{Perm}_{\mathcal{H}_A^{\otimes k}}(\sigma) . \tag{S8}$$

Since the above term is independent of z , the summation of these terms over z merely introduces a constant factor, which is absorbed in the normalization \mathcal{N} . The normalization is determined by the fact that the trace is unity. Defining

$$h_\sigma(\rho_0) = \text{Tr} \rho_0^{n_1} \dots \text{Tr} \rho_0^{n_{|\sigma|}} = \sum_{l_1 \dots l_{|\sigma|}} \lambda_{l_1}^{n_1} \dots \lambda_{l_{|\sigma|}}^{n_{|\sigma|}} , \tag{S9}$$

where $|\sigma|$ is the number of cycles and n_m is the order of the m^{th} cycle of σ with $\sum_{m=1}^{|\sigma|} n_m = k$, we obtain Eq. 17 and Eq. 18 of the End Matter.

The independence argument

From the translation invariance of the Haar measure, it is evident that the distribution of $U_A |\chi_{z,l}^A(U)\rangle \langle \chi_{z,l}^A(U)| U_A^\dagger$ is independent of the distribution of $|\chi_{z,l}^A(U)\rangle \langle \chi_{z,l}^A(U)|$, where $|\chi_{z,l}^A(U)\rangle := \frac{|\tilde{\chi}_{z,l}(U)\rangle}{\sqrt{\langle \tilde{\chi}_{z,l}(U) | \tilde{\chi}_{z,l}(U) \rangle}}$ is a normalised state. For $d \gg 1$, we show that

$$|\tilde{\chi}_{z,l}(U)\rangle \langle \tilde{\chi}_{z,l}(U)| \sim \frac{1}{d_B} |\chi_{z,l}^A(U)\rangle \langle \chi_{z,l}^A(U)| \tag{S10}$$

where $d_B = d/d_A$. This justifies that $U_A |\tilde{\chi}_{z,l}\rangle \langle \tilde{\chi}_{z,l}| U_A^\dagger$ is independent of U in the limit $d \rightarrow \infty$. To show Eq. S10, we prove that the distribution of $\langle \tilde{\chi}_{z,l} | \tilde{\chi}_{z,l} \rangle$ is sharply peaked around $1/d_B$ for $d \gg 1$ using Levy's lemma.

Consider a Haar random state $|\Phi\rangle$, where $|\Phi\rangle \sim \text{Haar}(d)$. We define $|\Phi_z\rangle := (I_A \otimes \langle z|_B) |\Phi\rangle$ and $G(|\Phi\rangle) := \langle \Phi_z | \Phi_z \rangle$. Note that $G(|\Phi\rangle) = \langle \tilde{\chi}_{z,l} | \tilde{\chi}_{z,l} \rangle$. A quick calculation yields $\mathbb{E}_{|\Phi\rangle \sim \text{Haar}(d)} G(|\Phi\rangle) = d_B^{-1}$. We now state Levy's lemma.

Lemma 1. (Levy's lemma for random states, see [26]) *Let $f : \mathbb{S}^{2d-1} \rightarrow \mathbb{R}$ be an η -Lipschitz function. Then for any $\delta \geq 0$, we have*

$$\text{Prob}_{|\Phi\rangle \sim \text{Haar}(d)} [|f(|\Phi\rangle) - \mathbb{E}_{|\Psi\rangle \sim \text{Haar}(d)} [f(|\Psi\rangle)]| \geq \delta] \leq 2 \exp\left(-\frac{2d\delta^2}{9\pi^3\eta^2}\right) \quad (\text{S11})$$

Borrowing the notational framework from [26], given $\vec{v} \in \mathbb{S}^{2d-1}$, we have $|\Phi\rangle = [I_d \ iI_d] \cdot \vec{v}$, where $|\Phi\rangle$ is a normalised state in \mathbb{C}^d and I_d is a $d \times d$ identity matrix. This allows us to represent the arguments of f either as normalised states in \mathbb{C}^d or real vectors in \mathbb{S}^{2d-1} . Here, \vec{v} is represented as $\begin{bmatrix} \vec{a} \\ \vec{b} \end{bmatrix}$, where $\vec{a}, \vec{b} \in \mathbb{R}^d$ and $\vec{a} \cdot \vec{a} + \vec{b} \cdot \vec{b} = 1$. To apply Levy's lemma to $G(|\Phi\rangle)$, we prove the following lemma:

Lemma 2. A Lipschitz constant for G is $\eta = 2$.

Proof. Since G is a differentiable function, we can take any η such that

$$\eta \geq \left\| \frac{d}{d\vec{v}} G(|\Phi\rangle) \right\|_2$$

We have

$$\begin{aligned} \left\| \frac{d}{d\vec{v}} G(|\Phi\rangle) \right\|_2 &= \left\| \frac{d}{d\vec{v}} \left(\vec{v}^\top \cdot \begin{bmatrix} \mathbb{I} \\ -i\mathbb{I} \end{bmatrix} \cdot (I_A \otimes |z\rangle \langle z|_B) \cdot \begin{bmatrix} \mathbb{I} & i\mathbb{I} \end{bmatrix} \cdot \vec{v} \right) \right\|_2 \\ &= \left\| \begin{bmatrix} 2P_z & \mathbb{O} \\ \mathbb{O} & 2P_z \end{bmatrix} \cdot \vec{v} \right\|_2 \\ &= 2 \left(\vec{a} \cdot P_z \cdot \vec{a} + \vec{b} \cdot P_z \cdot \vec{b} \right) \leq 2 \end{aligned}$$

where $P_z = \mathbb{I}_A \otimes |z\rangle \langle z|_B$ and \mathbb{O} and \mathbb{I} are $d \times d$ null and identity matrices, respectively. Combining this result with Lemma 1 gives us the concentration inequality:

$$\text{Prob}_{|\Phi\rangle \sim \text{Haar}(d)} \left[\left| G(|\Phi\rangle) - \frac{1}{d_B} \right| \geq \delta \right] \leq 2 \exp\left(-\frac{d\delta^2}{18\pi^3}\right) \quad (\text{S12})$$

which concludes the justification for the independence argument.

II. TYPICALITY OF $\mathcal{E}_{\text{ref}}[\rho_0]$ OVER RANDOM UNITARIES

In this section, we provide evidence for the argument that the moments of $\mathcal{E}_{\text{ref}}[\rho_0]$ computed by averaging over $U \sim \text{Haar}(d)$ is typical of $\text{Haar}(d)$ for large d . To this end, we demonstrate that the distribution of each component of the moments of the projected of the ensemble in some basis is strongly concentrated about its Haar-averaged value for $d \gg 1$. The key to this argument is Levy's lemma for a random unitary, stated as follows:

Lemma 3. (Levy's lemma for a random unitary, see [53]) *Let f be an η -Lipschitz function on $U(d)$. Then for any $\delta \geq 0$, we have*

$$\text{Prob}_{U \sim \text{Haar}(d)} [|f(U) - \mathbb{E}_{V \sim \text{Haar}(d)} [f(V)]| \geq \delta] \leq 4 \exp\left(-\frac{2d\delta^2}{9\pi^3\eta^2}\right). \quad (\text{S13})$$

We will now define the function of interest to apply this lemma to the projected ensemble of the form in [eq (1)]. Following the notations from Appx. F of [26], we define $|i\rangle = \otimes_{k=1}^t |i^{(k)}\rangle$ and $|j\rangle = \otimes_{k=1}^t |j^{(k)}\rangle$, where each

$|i^{(k)}\rangle, |j^{(k)}\rangle \in \mathcal{H}_A$. Consider the function $f_{ij} : U(d) \rightarrow \mathbb{R}$ defined by

$$\begin{aligned} f_{ij}(U) &= \sum_{z_B} \langle i | \left(\frac{(\sum_m \lambda_m |\tilde{\chi}_{z,m}\rangle \langle \tilde{\chi}_{z,m}|)^{\otimes k}}{(\sum_m \lambda_m \langle \tilde{\chi}_{z,m} | \tilde{\chi}_{z,m}\rangle)^{k-1}} \right) | j \rangle \\ &= \sum_{z_B} \frac{\prod_{l=1}^k \sum_{m_l} \lambda_{m_l} \langle i^{(l)} | \tilde{\chi}_{z,m_l}\rangle \langle \tilde{\chi}_{z,m_l} | j^{(l)}\rangle}{(\sum_m \lambda_m \langle \tilde{\chi}_{z,m} | \tilde{\chi}_{z,m}\rangle)^{k-1}}, \end{aligned} \quad (\text{S14})$$

where $|\tilde{\chi}_{z,m}\rangle = (\mathbb{I}_{D_A} \otimes \langle z_B |) U |m\rangle$ (defined in Sec. I) encodes the U dependence. We now prove the following lemma:

Lemma 4. A Lipschitz constant for f_{ij} is $\eta = 2(2k - 1)$.

Proof. Any η such that

$$\eta \geq \left\| \frac{d}{dU} f_{ij}(U) \right\|_2,$$

can be a Lipschitz constant since f_{ij} is differentiable. To obtain this bound, we express the above matrix derivative as an array of vector derivatives in a particular basis. To that end, we define $\vec{u}_m \in \mathbb{S}^{2d-1}$ such that $U |m\rangle = [\mathbb{I} \ i\mathbb{I}] \cdot \vec{u}_m$.

We express $\frac{d}{dU} f_{ij}(U)$ as $\left[\frac{d}{d\vec{u}_m} f_{ij}(U) \right]_m$, where \mathbb{I} denotes the $d \times d$ identity matrix. We have

$$\begin{aligned} \frac{d}{d\vec{u}_m} f_{ij}(U) &= \sum_{l'=1}^k \sum_z \frac{\prod_{l \neq l'} \sum_{m_l} \lambda_{m_l} \langle i^{(l)} | \tilde{\chi}_{z,m_l}\rangle \langle \tilde{\chi}_{z,m_l} | j^{(l)}\rangle}{(\sum_m \lambda_m \langle \tilde{\chi}_{z,m} | \tilde{\chi}_{z,m}\rangle)^{k-1}} \sum_{m_{l'}} \lambda_{m_{l'}} \frac{d}{d\vec{u}_m} \langle i^{(l')} | \tilde{\chi}_{z,m_{l'}}\rangle \langle \tilde{\chi}_{z,m_{l'}} | j^{(l')}\rangle \\ &\quad - (k-1) \sum_z \frac{\prod_{l=1}^k \sum_{m_l} \lambda_{m_l} \langle i^{(l)} | \tilde{\chi}_{z,m_l}\rangle \langle \tilde{\chi}_{z,m_l} | j^{(l)}\rangle}{(\sum_m \lambda_m \langle \tilde{\chi}_{z,m} | \tilde{\chi}_{z,m}\rangle)^k} \sum_n \lambda_n \frac{d}{d\vec{u}_m} \langle \tilde{\chi}_{z,n} | \tilde{\chi}_{z,n}\rangle \\ &= \sum_{l'=1}^k \sum_z \frac{\prod_{l \neq l'} \sum_{m_l} \lambda_{m_l} \langle i^{(l)} | \tilde{\chi}_{z,m_l}\rangle \langle \tilde{\chi}_{z,m_l} | j^{(l)}\rangle}{(\sum_m \lambda_m \langle \tilde{\chi}_{z,m} | \tilde{\chi}_{z,m}\rangle)^{k-1}} \left\{ \begin{bmatrix} M_{l'}^+ & -iM_{l'}^- \\ iM_{l'}^+ & M_{l'}^+ \end{bmatrix} \otimes |z\rangle \langle z|_B \right\} \cdot \vec{u}_m \lambda_m \\ &\quad - (k-1) \sum_z \frac{\prod_{l=1}^k \sum_{m_l} \lambda_{m_l} \langle i^{(l)} | \tilde{\chi}_{z,m_l}\rangle \langle \tilde{\chi}_{z,m_l} | j^{(l)}\rangle}{(\sum_m \lambda_m \langle \tilde{\chi}_{z,m} | \tilde{\chi}_{z,m}\rangle)^k} \begin{bmatrix} P_z & 0 \\ 0 & P_z \end{bmatrix} \cdot \vec{u}_m \times 2\lambda_m, \end{aligned} \quad (\text{S15})$$

where we have defined $M_{l'}^\pm = |i^{(l')}\rangle \langle j^{(l')}| \pm |j^{(l')}\rangle \langle i^{(l')}|$ and have explicitly evaluated the derivatives. This gives

$$\begin{aligned} \frac{d}{dU} f_{ij}(U) &= \sum_{l'=1}^k \sum_z \frac{\prod_{l \neq l'} \sum_{m_l} \lambda_{m_l} \langle i^{(l)} | \tilde{\chi}_{z,m_l}\rangle \langle \tilde{\chi}_{z,m_l} | j^{(l)}\rangle}{(\sum_m \lambda_m \langle \tilde{\chi}_{z,m} | \tilde{\chi}_{z,m}\rangle)^{k-1}} \left\{ \begin{bmatrix} M_{l'}^+ & -iM_{l'}^- \\ iM_{l'}^+ & M_{l'}^+ \end{bmatrix} \otimes |z\rangle \langle z|_B \right\} \cdot VD \\ &\quad - (k-1) \sum_z \frac{\prod_{l=1}^k \sum_{m_l} \lambda_{m_l} \langle i^{(l)} | \tilde{\chi}_{z,m_l}\rangle \langle \tilde{\chi}_{z,m_l} | j^{(l)}\rangle}{(\sum_m \lambda_m \langle \tilde{\chi}_{z,m} | \tilde{\chi}_{z,m}\rangle)^k} \begin{bmatrix} P_z & 0 \\ 0 & P_z \end{bmatrix} \cdot VD \times 2, \end{aligned} \quad (\text{S16})$$

where $V : \mathbb{C}^d \rightarrow \mathbb{S}^{2d-1}$ is a matrix such that $U = [\mathbb{I} \ i\mathbb{I}] \cdot V$ and $D = \text{dia}(\lambda_1, \lambda_2, \dots, \lambda_m)$. Taking the norm and applying the triangle inequality gives

$$\begin{aligned} \left\| \frac{d}{dU} f_{ij}(U) \right\|_2 &\leq \left\| \sum_{l'=1}^k \sum_z \frac{\prod_{l \neq l'} \sum_{m_l} \lambda_{m_l} \langle i^{(l)} | \tilde{\chi}_{z,m_l}\rangle \langle \tilde{\chi}_{z,m_l} | j^{(l)}\rangle}{(\sum_m \lambda_m \langle \tilde{\chi}_{z,m} | \tilde{\chi}_{z,m}\rangle)^{k-1}} \left\{ \begin{bmatrix} M_{l'}^+ & -iM_{l'}^- \\ iM_{l'}^+ & M_{l'}^+ \end{bmatrix} \otimes |z\rangle \langle z|_B \right\} \cdot VD \right\|_2 \\ &\quad + 2(k-1) \left\| \sum_z \frac{\prod_{l=1}^k \sum_{m_l} \lambda_{m_l} \langle i^{(l)} | \tilde{\chi}_{z,m_l}\rangle \langle \tilde{\chi}_{z,m_l} | j^{(l)}\rangle}{(\sum_m \lambda_m \langle \tilde{\chi}_{z,m} | \tilde{\chi}_{z,m}\rangle)^k} \begin{bmatrix} P_z & 0 \\ 0 & P_z \end{bmatrix} \cdot VD \right\|_2, \end{aligned} \quad (\text{S17})$$

We now individually bound each of the terms on the RHS. For the first term, writing $b_{l',z} =$

$(\prod_{l \neq l'} \sum_{m_l} \lambda_{m_l} \langle i^{(l)} | \tilde{\chi}_{z, m_l} \rangle \langle \tilde{\chi}_{z, m_l} | j^{(l)} \rangle) / (\sum_m \lambda_m \langle \tilde{\chi}_{z, m} | \tilde{\chi}_{z, m} \rangle)^{k-1}$ and $M_{l'} = \begin{bmatrix} M_{l'}^\dagger & -iM_{l'}^- \\ iM_{l'}^+ & M_{l'}^\dagger \end{bmatrix}$, we have

$$\begin{aligned} \left\| \sum_{l'=1}^k \sum_z b_{l',z} \{M_{l'} \otimes |z\rangle \langle z|_B\} VD \right\|_2 &= \left(\sum_{l',p'=1}^k \sum_z b_{p',z}^* b_{l',z} \text{Tr} \left[DV^\dagger \left(M_{p'}^\dagger M_{l'} \otimes |z\rangle \langle z|_B \right) VD \right] \right)^{1/2} \\ &\leq \left(\sum_{l',p'=1}^k \sum_z |b_{p',z}^*| |b_{l',z}| \text{Tr} \left[DV^\dagger \left(|M_{p'}^\dagger M_{l'}| \otimes |z\rangle \langle z|_B \right) VD \right] \right)^{1/2}, \end{aligned} \quad (\text{S18})$$

where $|A| := \sqrt{A^\dagger A}$. We note that

$$\begin{aligned} |b_{l',z}| &= \left| \text{Tr} \left\{ \left(\otimes_{l \neq l'} |j^{(l)}\rangle \langle i^{(l)}| \right) \cdot \left(\frac{(\sum_m \lambda_m |\tilde{\chi}_{z,m}\rangle \langle \tilde{\chi}_{z,m}|)^{\otimes k-1}}{(\sum_m \lambda_m \langle \tilde{\chi}_{z,m} | \tilde{\chi}_{z,m} \rangle)^{k-1}} \right) \right\} \right| \\ &\leq \left\| \otimes_{l \neq l'} |j^{(l)}\rangle \langle i^{(l)}| \right\|_2 \left\| \frac{\sum_m \lambda_m |\tilde{\chi}_{z,m}\rangle \langle \tilde{\chi}_{z,m}|}{\sum_m \lambda_m \langle \tilde{\chi}_{z,m} | \tilde{\chi}_{z,m} \rangle} \right\|_2^{k-1} \leq 1, \end{aligned} \quad (\text{S19})$$

since $\left\| \otimes_{l \neq l'} |j^{(l)}\rangle \langle i^{(l)}| \right\|_2 = 1$ and

$$\left\| \frac{\sum_m \lambda_m |\tilde{\chi}_{z,m}\rangle \langle \tilde{\chi}_{z,m}|}{\sum_m \lambda_m \langle \tilde{\chi}_{z,m} | \tilde{\chi}_{z,m} \rangle} \right\|_2 = \left(\frac{\sum_{m,m'} \lambda_m \lambda_{m'} |\langle \tilde{\chi}_{z,m} | \tilde{\chi}_{z,m'} \rangle|^2}{\sum_{m,m'} \lambda_m \lambda_{m'} \langle \tilde{\chi}_{z,m} | \tilde{\chi}_{z,m} \rangle \langle \tilde{\chi}_{z,m'} | \tilde{\chi}_{z,m'} \rangle} \right) \leq 1, \quad (\text{S20})$$

where the inequality follows from the Cauchy-Schwarz inequality. Eq. S18 is less than or equal to

$$\begin{aligned} \left(\sum_{l',p'=1}^k \sum_z \text{Tr} \left[DV^\dagger \left(|M_{p'}^\dagger M_{l'}| \otimes |z\rangle \langle z|_B \right) VD \right] \right)^{1/2} &= \left(\sum_{l',p'=1}^k \text{Tr} \left[DV^\dagger \left(|M_{p'}^\dagger M_{l'}| \otimes \mathbb{I}_B \right) VD \right] \right)^{1/2} \\ &= \left(\sum_{l',p'=1}^k \sum_m \lambda_m^2 \vec{u}_m^T \cdot \left(|M_{p'}^\dagger M_{l'}| \otimes \mathbb{I}_B \right) \cdot \vec{u}_m \right)^{1/2} \\ &\leq \left(\sum_{l',p'=1}^k \|M_{p'}^\dagger M_{l'}\|_\infty \right)^{1/2}, \end{aligned} \quad (\text{S21})$$

where we have used the monotonicity of norms and that $\lambda_m \in [0, 1]$ with $\sum_m \lambda_m = 1$, in addition to $\vec{u}_m^T \cdot \vec{u}_m = 1$. Since $\|M_{p'}^\dagger M_{l'}\|_\infty \leq \|M_{p'}^\dagger\|_\infty \|M_{l'}\|_\infty \leq 4$, the above is $\leq 2k$.

Now we bound the second term in the RHS of Eq. S17. Letting $c_z = \left(\prod_{l=1}^k \sum_{m_l} \lambda_{m_l} \langle i^{(l)} | \tilde{\chi}_{z, m_l} \rangle \langle \tilde{\chi}_{z, m_l} | j^{(l)} \rangle \right) / (\sum_m \lambda_m \langle \tilde{\chi}_{z, m} | \tilde{\chi}_{z, m} \rangle)^k$, the term can be written as

$$2(k-1) \left(\sum_z |c_z|^2 \text{Tr} \left[DV^\dagger \cdot \begin{bmatrix} P_z & 0 \\ 0 & P_z \end{bmatrix} \cdot VD \right] \right)^{1/2} = 2(k-1) \left(\sum_z |c_z|^2 \sum_m \lambda_m^2 \vec{u}_m^T \cdot \begin{bmatrix} P_z & 0 \\ 0 & P_z \end{bmatrix} \cdot \vec{u}_m \right)^{1/2}. \quad (\text{S22})$$

Using the bound

$$\begin{aligned} |c_z| &= \left| \text{Tr} \left\{ \left(\otimes_{l \neq l'} |j^{(l)}\rangle \langle i^{(l)}| \right) \cdot \left(\frac{(\sum_m \lambda_m |\tilde{\chi}_{z,m}\rangle \langle \tilde{\chi}_{z,m}|)^{\otimes k}}{(\sum_m \lambda_m \langle \tilde{\chi}_{z,m} | \tilde{\chi}_{z,m} \rangle)^k} \right) \right\} \right| \\ &\leq \left\| \otimes_{l \neq l'} |j^{(l)}\rangle \langle i^{(l)}| \right\|_2 \left\| \frac{\sum_m \lambda_m |\tilde{\chi}_{z,m}\rangle \langle \tilde{\chi}_{z,m}|}{\sum_m \lambda_m \langle \tilde{\chi}_{z,m} | \tilde{\chi}_{z,m} \rangle} \right\|_2^k \leq 1, \end{aligned} \quad (\text{S23})$$

we can upper bound Eq. S22 by

$$\begin{aligned} 2(k-1) \left(\sum_z \sum_m \lambda_m^2 \vec{u}_m^T \cdot \begin{bmatrix} P_z & 0 \\ 0 & P_z \end{bmatrix} \cdot \vec{u}_m \right)^{1/2} &= 2(k-1) \left(\sum_z \sum_m \lambda_m^2 \vec{u}_m^T \cdot \left(\begin{bmatrix} \mathbb{I}_A & 0 \\ 0 & \mathbb{I}_A \end{bmatrix} \otimes P_z \right) \cdot \vec{u}_m \right)^{1/2} \\ &\leq 2(k-1). \end{aligned} \quad (\text{S24})$$

Putting our bounds together, we have

$$\left\| \frac{d}{dU} f_{ij}(U) \right\|_2 \leq 2k + 2(k-1) = 2(2k-1). \quad (\text{S25})$$

which concludes our proof of Lemma 4. Combining this result with Lemma 3, we obtain the concentration inequality:

$$\text{Prob}_{U \sim \text{Haar}(d)} [|f_{ij}(U) - \mathbb{E}_{V \sim \text{Haar}(d)} [f_{ij}(V)]| \geq \delta] \leq 4 \exp \left(-\frac{d\delta^2}{18\pi^3(2k-1)^2} \right), \quad (\text{S26})$$

which explicitly shows typicality for $d \gg 1$.

III. CONNECTION TO THE SCROOGE ENSEMBLE

In this section, we prove the relation in Eq. 10, which demonstrates that $\mathcal{E}_{\text{ref}}[\rho_0]$ can be obtained by partially tracing out states from an appropriately defined Scrooge ensemble. We first lay out a few definitions for notational convenience. The computational basis of the Hilbert space of $A \cup B$ (or of the Hilbert space of X) is given by $\{|l\rangle\}_{l=1}^{D_X}$. We now define the kets

$$\begin{aligned} |\tilde{\chi}_{z,l}\rangle &:= (\mathbb{I}_{D_A} \otimes \langle z_B |) U |l\rangle \\ |\tilde{\psi}_z\rangle &:= \sum_l |l\rangle \otimes |\tilde{\chi}_{z,l}\rangle, \end{aligned} \quad (\text{S27})$$

where $U \sim \text{Haar}(D_{AB})$. This enables a compact representation of the states $|\phi_{XA}(z_B)\rangle$ and the probabilities $p(z_B)$, such that

$$|\phi_{XA}(z_B)\rangle = \frac{\sqrt{\rho_{XA}} |\tilde{\psi}_z\rangle}{\sqrt{\langle \tilde{\psi}_z | \rho_{XA} | \tilde{\psi}_z \rangle}} \quad (\text{S28})$$

$$p(z_B) = D_A \langle \tilde{\psi}_z | \rho_{XA} | \tilde{\psi}_z \rangle,$$

where $\rho_{XA} = (\rho_0^T \otimes \mathbb{I}_{D_A}) / D_A$. The moments of $\mathcal{E}_{\text{ref}}[\rho_0]$ are given by

$$\begin{aligned} \rho_{\mathcal{E}_{\text{ref}}[\rho_0]}^{(k)} &= \sum_{z_B} p(z_B) [\text{Tr}_X |\phi_{XA}(z_B)\rangle \langle \phi_{XA}(z_B)|]^{otimes k} \\ &= \sum_{z_B} \int dU_{\text{Haar}(D_{AB})} D_A \frac{\left(\text{Tr}_X \left[\sqrt{\rho_{XA}} |\tilde{\psi}_z\rangle \langle \tilde{\psi}_z | \sqrt{\rho_{XA}} \right] \right)^{otimes k}}{\langle \tilde{\psi}_z | \rho_{XA} | \tilde{\psi}_z \rangle^{k-1}}, \end{aligned} \quad (\text{S29})$$

where the Haar integral appears due to typicality in the limit $D_B \rightarrow \infty$. We note that the distribution of $\langle \tilde{\psi}_z | \tilde{\psi}_z \rangle$ is highly concentrated around D_A in the limit $D_B \rightarrow \infty$ (this follows from the concentration of $\langle \tilde{\chi}_{z,l} | \tilde{\chi}_{z,l} \rangle$, which was proven in Sec. I). This allows us to plug in the normalised state $|\psi_z\rangle = \frac{|\tilde{\psi}_z\rangle}{\sqrt{\langle \tilde{\psi}_z | \tilde{\psi}_z \rangle}}$ into Eq. S29, giving

$$\rho_{\mathcal{E}_{\text{ref}}[\rho_0]}^{(k)} = \sum_{z_B} \int dU_{\text{Haar}(D_{AB})} D_A^2 \frac{\left(\text{Tr}_X \left[\sqrt{\rho_{XA}} |\psi_z\rangle \langle \psi_z | \sqrt{\rho_{XA}} \right] \right)^{otimes k}}{\langle \psi_z | \rho_{XA} | \psi_z \rangle^{k-1}}. \quad (\text{S30})$$

Now, we prove that the continuous set $\mathcal{E}_U = \{dU_{\text{Haar}(D_{AB})}, |\psi_z\rangle\}$ forms an exact state k -design (for a fixed k) over $\mathbb{C}^{D_{XA}}$ in the limit $D_B \rightarrow \infty$. The moments of \mathcal{E}_U are given by

$$\begin{aligned} \rho_{\mathcal{E}_U}^{(k)} &= \int dU_{\text{Haar}(D_{AB})} (|\psi_z\rangle \langle \psi_z|)^{otimes k} \\ &= \int dU_{\text{Haar}(D_{AB})} \frac{\left(\sum_{l,l'} |l'\rangle \langle l| \otimes |\tilde{\chi}_{z,l'}\rangle \langle \tilde{\chi}_{z,l}| \right)^{otimes k}}{\left(\sum_l \langle \tilde{\chi}_{z,l} | \tilde{\chi}_{z,l} \rangle \right)^k}. \end{aligned} \quad (\text{S31})$$

The above integral is invariant under the transformation $U \rightarrow (U_A \otimes \mathbb{I}_{D_B})U$, where $U_A \sim \text{Haar}(D_A)$ is statistically independent of U . Plugging this into Eq. S31

$$\rho_{\mathcal{E}_U}^{(k)} = \int dU_{A, \text{Haar}(D_A)} \int dU_{\text{Haar}(D_{AB})} \frac{\left(\sum_{l, l'} |l\rangle \langle l| \otimes \left(U_A |\tilde{\chi}_{z, l'}\rangle \langle \tilde{\chi}_{z, l'}| U_A^\dagger \right) \right)^{\otimes k}}{\left(\sum_l \langle \tilde{\chi}_{z, l} | \tilde{\chi}_{z, l} \rangle \right)^k}. \quad (\text{S32})$$

The above integral factorises since $U_A |\tilde{\chi}_{z, l}\rangle \langle \tilde{\chi}_{z, l}| U_A^\dagger$ is statistically independent of U in the limit of $D_B \rightarrow \infty$ (see proof in Sec. I). In addition, $U_A |\tilde{\chi}_{z, l}\rangle$ is identically distributed to $|\tilde{\zeta}_{z, l}\rangle := (\mathbb{I}_{D_A} \otimes \langle z_B |) V |l\rangle$, where $V \sim \text{Haar}(D_{AB})$. This gives

$$\begin{aligned} \rho_{\mathcal{E}_U}^{(k)} &= \int dV_{\text{Haar}(D_{AB})} \left(\sum_{l, l'} |l'\rangle \langle l| \otimes |\tilde{\zeta}_{z, l'}\rangle \langle \tilde{\zeta}_{z, l}| \right)^{\otimes k} \int dU_{\text{Haar}(D_{AB})} \left(\sum_l \langle \tilde{\chi}_{z, l} | \tilde{\chi}_{z, l} \rangle \right)^{-k} \\ &= \mathcal{N} \sum_{\substack{l_1 \dots l_k \\ l'_1 \dots l'_k}} \left(|l'_1\rangle \langle l_1| \otimes \dots \otimes |l'_k\rangle \langle l_k| \otimes \sum_{\sigma, \tau \in S_k} \left(\text{Wg}(\sigma\tau^{-1}, D_{AB}) \delta_{l'_1, l_{\tau(1)}} \dots \delta_{l'_k, l_{\tau(k)}} \text{Perm}_{\mathcal{H}_A^{\otimes k}}(\sigma) \right) \right) \\ &= \mathcal{N} \sum_{\sigma \in S_k} \sum_{l_1 \dots l_k} |l_{\sigma(1)}\rangle \langle l_1| \otimes \dots \otimes |l_{\sigma(k)}\rangle \langle l_k| \otimes \text{Perm}_{\mathcal{H}_A^{\otimes k}}(\sigma) \\ &= \frac{\sum_{\sigma \in S_k} \text{Perm}(\mathcal{H}_X \otimes \mathcal{H}_A)^{\otimes k}(\sigma)}{D_{AX}(D_{AX} + 1) \dots (D_{AX} + k - 1)}, \end{aligned} \quad (\text{S33})$$

where the intermediate equalities hold modulo an ordering of the tensor products. The integral in the right of the first line of Eq. S33 is absorbed by a normalisation constant \mathcal{N} , which can be evaluated by taking the trace of the numerator in the last line of Eq. S33. Since \mathcal{E}_U forms an exact state t -design over $\mathbb{C}^{D_{XA}}$, the integral $\int_{U \sim \text{Haar}(D_{AB})}$ in Eq. S30 can be replaced with the integral $\int d\psi_{\text{Haar}(D_{XA})}$ (see Sec. VI of Supp. Matt. of [27] for a detailed justification) and ψ_z with ψ , which gives us

$$\begin{aligned} \rho_{\mathcal{E}_{\text{ref}}[\rho_0]}^{(k)} &= \sum_{z_B} \int d\psi_{\text{Haar}(D_{XA})} D_A^2 \frac{(\text{Tr}_X [\sqrt{\rho_{XA}} |\psi\rangle \langle \psi| \sqrt{\rho_{XA}}])^{\otimes k}}{\langle \psi | \rho_{XA} | \psi \rangle^{k-1}} \\ &= \int d\psi_{\text{Haar}(D_{XA})} D_{XA} \frac{(\text{Tr}_X [\sqrt{\rho_{XA}} |\psi\rangle \langle \psi| \sqrt{\rho_{XA}}])^{\otimes k}}{\langle \psi | \rho_{XA} | \psi \rangle^{k-1}}, \end{aligned} \quad (\text{S34})$$

which is Eq. 10 of the main text.

IV. CONDITIONS FOR $\mathcal{E}_{\text{ref}}[\rho_0]$ TO REDUCE TO THE GENERALIZED HILBERT-SCHMIDT ENSEMBLE

In this section, we explicitly demonstrate how $\mathcal{E}_{\text{ref}}[\rho_0]$ reduces to an appropriate gHSe (at the level of their respective moments) under the conditions that were laid out in the main text. The gHSe is defined by tracing out subsystem R from Haar random states on $R \cup A$,

$$\mathcal{E}_{\text{gHSe}} = \{ \text{Tr}_R[|\psi\rangle \langle \psi|] : |\psi\rangle \sim \text{Haar}(D_{RA}) \}, \quad (\text{S35})$$

The moments of $\mathcal{E}_{\text{ref}}[\rho_0]$ reduce to those of $\mathcal{E}_{\text{gHSe}}$ (with $D_R = \text{rank}(\rho_0)$) if the non-zero part of the spectrum of ρ_0 is flat. Under this condition, the moments of $\mathcal{E}_{\text{ref}}[\rho_0]$ acquire a simple form, which we obtain by plugging in $\text{Tr}\rho_0^n = D_R^{1-n}$ into Eq. S8,

$$\begin{aligned} \rho_{\mathcal{E}_{\text{ref}}[\rho_0]}^{(k)} &= \frac{\sum_{\sigma \in S_k} D_R^{1-n_1} \dots D_R^{1-n_{|\sigma|}} \text{Perm}_{\mathcal{H}_A^{\otimes k}}(\sigma)}{\sum_{\sigma \in S_k} D_R^{1-n_1} \dots D_R^{n_1-|\sigma|} D_A^{|\sigma|}} \\ &= \frac{\sum_{\sigma \in S_k} D_R^{|\sigma|} \text{Perm}_{\mathcal{H}_A^{\otimes k}}(\sigma)}{\sum_{\sigma \in S_k} D_{RA}^{|\sigma|}} \end{aligned} \quad (\text{S36})$$

where we used the identity $\sum_i^{|\sigma|} n_i = k$. This exactly matches with the corresponding moment of the gHSe which, according to Eq. S35, is given by,

$$\begin{aligned} \rho_{\mathcal{E}_{\text{gHSe}}}^{(k)} &= \int d\psi_{\text{Haar}(D_{RA})} (\text{Tr}_R [|\psi\rangle\langle\psi|])^{\otimes k} \\ &= \frac{\sum_{\sigma \in S_k} \text{Tr} \left[\text{Perm}_{\mathcal{H}_R^{\otimes k}}(\sigma) \right] \text{Perm}_{\mathcal{H}_A^{\otimes k}}(\sigma)}{\sum_{\sigma \in S_k} D_{RA}^{|\sigma|}} \\ &= \frac{\sum_{\sigma \in S_k} D_R^{|\sigma|} \text{Perm}_{\mathcal{H}_A^{\otimes k}}(\sigma)}{\sum_{\sigma \in S_k} D_{RA}^{|\sigma|}} \end{aligned} \quad (\text{S37})$$

where the intermediate equalities hold modulo an ordering of the tensor products.

V. FINITE-SIZE SCALING AND DEEP-THERMALISATION TIMESCALES FOR THE KICKED ISING CHAIN

In this section, we provide additional details of the finite-size scaling analysis for $\Delta_k(t)$ for the kicked Ising chain and also the extraction of the deep-thermalisation timescale t_k shown in Fig. 3. To start, we first show the raw data for $\Delta_k(t)$ as a function of t for different system sizes L and for different $|S|$, which in turn controls the mixedness of the initial state.

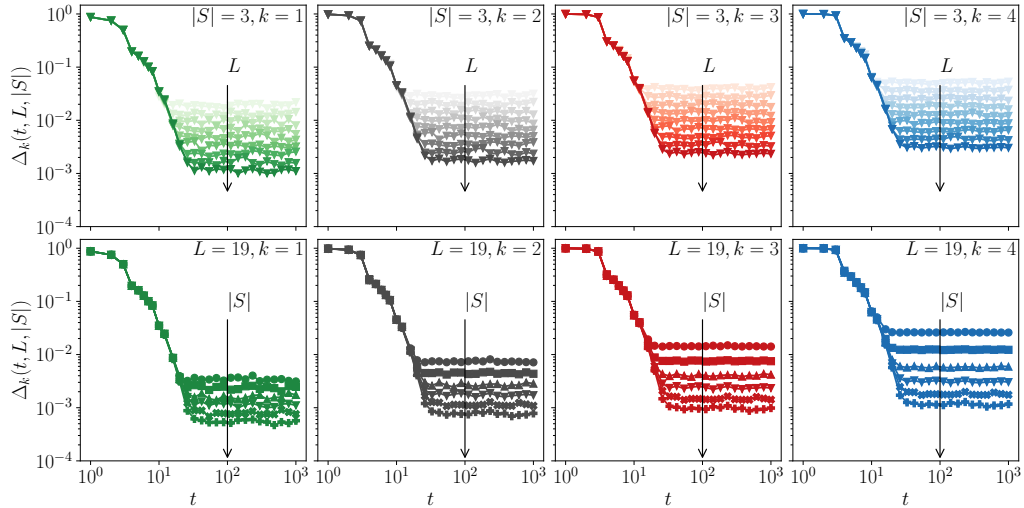


FIG. S1. Raw data for $\Delta_k(t, L, |S|)$ in the KIC. Top panels: fixed $|S| = 3$ and varying total sizes $L = 11, 12, \dots, 19$ (increasing intensity corresponds to larger L , as indicated by the arrows). Bottom panels: fixed $L = 19$ and varying $|S| = 1, 2, \dots, 6$ (different symbols; trend with $|S|$ shown by the arrow).

The data is shown in Fig. S1. The top panels shows representative data for $\Delta_k(t)$ as a function of t for fixed $|S|$ and varying total size L , while the bottom panels display $\Delta_k(t)$ for fixed L and varying $|S|$. One immediately observes that the finite-size saturation value (which decays with L) depends on both L and $|S|$, whereas the temporal profile prior to saturation is fully converged with them. This motivates the scaling form

$$\Delta_k(t, L, |S|) = f_k(L, |S|) g_k \left(\frac{t}{t_{\text{sat},k}(L, |S|)} \right), \quad (\text{S38})$$

with $g_k(x) \rightarrow 1$ for $x \gg 1$, implying

$$\Delta_k(t, L, |S|) = \begin{cases} C(t), & t \ll t_{\text{sat},k}(L, |S|), \\ f_k(L, |S|), & t \gg t_{\text{sat},k}(L, |S|), \end{cases} \quad (\text{S39})$$

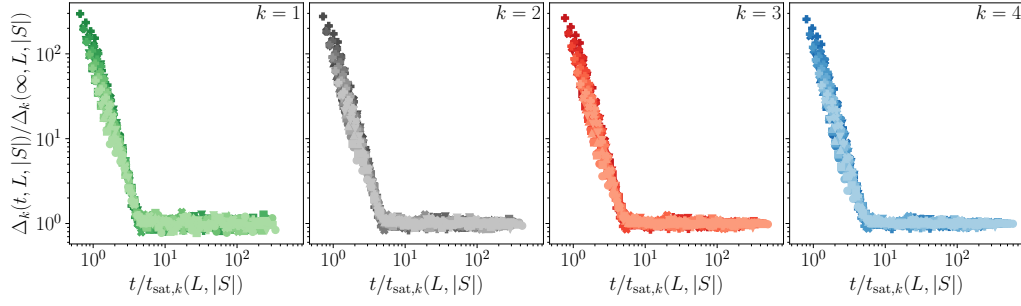


FIG. S2. Scale collapse of the data in Fig. S1 for different L and $|S|$, shown separately for each k . The excellent quality of the collapse supports the scaling form in Eq. S38.

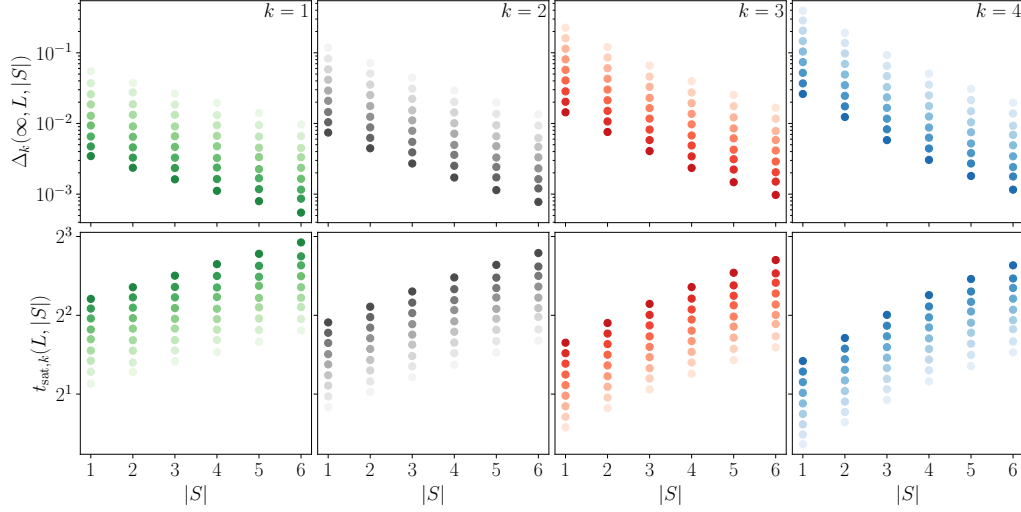


FIG. S3. Dependence of $\Delta_k(\infty, L, |S|)$ (top) and $t_{\text{sat},k}$ (bottom), which underlie the scaling collapse in Fig. S2, on $|S|$ and L . The data suggest that $\Delta_k(\infty, L, |S|)$ decays, while $t_{\text{sat},k}$ grows, with both $|S|$ and L .

where $t_{\text{sat},k}$ denotes the finite-size saturation time. Evidence for the validity of the scaling form in Eq. S38 is shown by the scale-collapsed data in Fig. S2. It is worth noting that $t_{\text{sat},k}$ is not the deep-thermalisation timescale, which is defined in the thermodynamic limit.

Two key conclusions follow from this analysis:

- The saturation value decays exponentially with both L and $|S|$,

$$f_k(L, |S|) \equiv \Delta_k(t \rightarrow \infty, L, |S|) \sim e^{-\alpha_k L - \beta_k |S|}. \quad (\text{S40})$$

This is evident from the data in the top panels of Fig. S3, where $\Delta_k(\infty, L, |S|)$ decreases linearly with $|S|$ on a semilogarithmic scale, indicating exponential decay with $|S|$; the curves for linearly spaced L values are similarly equispaced on logarithmic scales, indicating exponential decay with L as well.

- The saturation time $t_{\text{sat},k}$ diverges with L , implying that in the thermodynamic limit $\Delta_k(t, L, |S|)$ becomes independent of $|S|$. Hence, the deep-thermalisation timescale is an intrinsic property of the system and does not depend on the mixed-state partition. This is likewise evident from the bottom panels in Fig. S3.

To estimate t_k , we follow standard practice by defining it as the time when Δ_k falls below a threshold ϵ . The resulting t_k values, shown in Fig. 3 (in the End Matter), exhibit a weak monotonic growth consistent with both logarithmic and sub-linear power-law scaling with k . However, with the current limitations on our numerical calculations, it is not possible for us to unambiguously distinguish between the two cases.

Defining the product of the unitaries enclosed in the yellow boxes in the above equation as,

$$\mathcal{U}(z_{B \cap E}) := U(z_1)U(z_2)\dots U(z_{|B \cap E|}), \quad (\text{S45})$$

the unnormalised state can be written as

$$|\tilde{\psi}_{XA,t}(z_B)\rangle = \frac{1}{\sqrt{2^{|B|-|S|}}} \left(\sqrt{\rho_S^T} \otimes I_A \right) W(z_{B \cap S}) \mathcal{U}(z_{B \cap E}) |+\rangle^{\otimes t}, \quad (\text{S46})$$

where $W(z_{B \cap S})$ is a linear map from $\mathbb{C}^{2^t} \rightarrow \mathbb{C}^{2^{|A|+|S|}}$. Plugging this into Eq. S43, we obtain

$$\rho_{\mathcal{E}_{PE}}^{(k)} = \sum_{z_B} \frac{1}{2^{|B|}} \frac{(\text{Tr}_X[(\sqrt{\rho_S^T} \otimes I_A) W(z_{B \cap S}) \mathcal{U}(z_{B \cap E}) (|+\rangle \langle +|^{\otimes t}) \mathcal{U}(z_{B \cap E})^\dagger W(z_{B \cap S})^\dagger (\sqrt{\rho_S^T} \otimes I_A)])^{\otimes k}}{((|+\rangle \langle +|^{\otimes t} \mathcal{U}(z_{B \cap E})^\dagger W(z_{B \cap S})^\dagger (\rho_S^T \otimes I_A) W(z_{B \cap S}) \mathcal{U}(z_{B \cap E}) |+\rangle \langle +|^{\otimes t}))^{k-1}} \times 2^{|S|}. \quad (\text{S47})$$

For $t \geq |A| + |S|$, the map $W(z_{B \cap S})$ is expressible as

$$W(z_{B \cap S}) = \sqrt{2}^{(t-|A|-|S|)} |+\rangle^{\otimes (t-|A|-|S|)} V(z_{B \cap S}), \quad (\text{S48})$$

where $V(z_{B \cap S})$ is a unitary on \mathbb{C}^{2^t} whose particular form is unimportant. This is made explicit by the diagrammatic notation

(S49)

The diagram on the right hand side of the above equation follows trivially from the left hand side by rotating the wordlines and the gates about the corresponding dashed (red and blue) lines.

The second key feature of the SDKI is that the products of unitary matrices $U_{z_{B_i}}$ sample uniformly the space of unitaries in \mathbb{C}^{2^t} [27], which enable the analytic computation of the moments. In particular, in the limit of $|B \cap E| \rightarrow \infty$, Theorem 2 in Ref. [27] states that $\forall g/ \in Z\pi/8$

$$\lim_{|B \cap E| \rightarrow \infty} \sum_{z_{B \cap E}} \frac{1}{2^{|B \cap E|}} \mathcal{U}(z_{B \cap E})^{\otimes k} \otimes \mathcal{U}(z_{B \cap E})^{*\otimes k} = \int dU_{\text{Haar}(2^t)} U^{\otimes k} \otimes U^{*\otimes k}. \quad (\text{S50})$$

This enables us to replace the sum over states $\mathcal{U}(z_B) |+\rangle^{\otimes t}$ in Eq. S47 with the integral over the Haar random states $\Psi \sim \text{Haar}(2^t)$. The unitary $V(z_{B \cap S})$ can be absorbed in the Haar integral via invariance of the Haar measure.

Defining $|\Psi_+\rangle := \langle + |^{\otimes(t-|A|-|S|)} |\Psi\rangle$ and $|\Psi'\rangle := \frac{|\Psi_+\rangle}{\| |\Psi_+\rangle \|}$ and $\rho_{XA} = \rho_S^T \otimes I_A / 2^{|A|}$, the moments in the $|B \cap E| \rightarrow \infty$ limit can be conveniently expressed as

$$\begin{aligned} \lim_{|B \cap E| \rightarrow \infty} \rho_{\mathcal{E}_{PE}}^{(k)} &= \int d\Psi_{\text{Haar}(2^t)} \frac{(\text{Tr}_X [(\sqrt{\rho_{XA}} |\Psi_+\rangle \langle \Psi_+| \sqrt{\rho_{XA}})])^{\otimes k}}{\langle \Psi_+ | \rho_{XA} | \Psi_+ \rangle^{k-1}} \times 2^t \\ &= \int d\Psi_{\text{Haar}(2^t)} \frac{(\text{Tr}_X [\sqrt{\rho_{XA}} |\Psi'\rangle \langle \Psi'| \sqrt{\rho_{XA}}])^{\otimes k}}{\langle \Psi' | \rho_{XA} | \Psi' \rangle^k} \times 2^t \langle \Psi' | \rho_{XA} | \Psi' \rangle \times \langle \Psi_+ | \Psi_+ \rangle. \end{aligned} \quad (\text{S51})$$

Lemma 4 of [26] states that $|\Psi'\rangle$ and $\langle \Psi_+ | \Psi_+ \rangle$ are independent random variables, yielding

$$\begin{aligned} \lim_{|B \cap E| \rightarrow \infty} \rho_{\mathcal{E}_{PE}}^{(k)} &= \int d\Psi'_{\text{Haar}(2^t)} \frac{(\text{Tr}_X [\sqrt{\rho_{XA}} |\Psi'\rangle \langle \Psi'| \sqrt{\rho_{XA}}])^{\otimes k}}{\langle \Psi' | \rho_{XA} | \Psi' \rangle^k} \times 2^{|A|+|S|} \langle \Psi' | \rho_{XA} | \Psi' \rangle \\ &\quad \times \int d\Psi_{\text{Haar}(2^t)} 2^{t-|A|-|S|} \langle \Psi_+ | \Psi_+ \rangle \end{aligned} \quad (\text{S52})$$

where the latter integral is unity, thus giving the result in the main text.

VII. RESULTS FOR THE FLOQUET MIXED-FIELD ISING CHAIN

In the main text, our results, both numerical and analytical, were presented for the non-integrable kicked Ising chain (KIC) and at its self-dual point. While the non-integrable KIC is an archetypal model for chaotic/ergodic unitary dynamics, for the sake of generality (and completeness) we also present results here for the Floquet mixed-field Ising chain (FMFIC) with the measurements performed in a basis other than the computational basis. The Floquet unitary of the FMFIC is as

$$U_F = e^{-iH_+} e^{-iH_-}, \quad \text{with} \quad H_{\pm} = \sum_{i=1}^N [h_z(1 \pm \delta) Z_i + h_x X_i + J Z_i Z_{i+1}], \quad (\text{S53})$$

In this model, both steps of the Floquet period include Ising interactions as well as *both* transverse and longitudinal fields. As such, it cannot be recast as a reparametrisation of the KIC. Moreover, the projected ensemble is generated by measurements of $\{Y_i : i \in B\}$, which are, by construction, not in the computational basis.

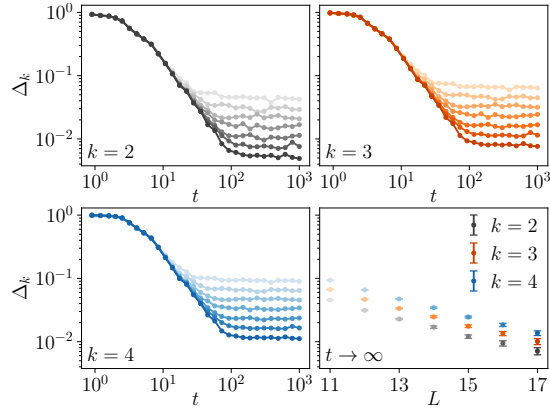


FIG. S4. Results for $\Delta_k(t)$ for the FMFIC with parameters $(h_z, h_x, J, \delta, T) = (0.8090, 0.9045, 1, 0.5, 1)$. The subsystem size $|A| = 3$ is fixed, while different intensities correspond to $|B| = 8, 10, \dots, 14$, with darker colours denoting larger values. The initial state is of the form in Eq. 13 with ρ_S a maximally mixed state with $|S| = 3$. The results are, qualitatively, indistinguishable from those for the KIC shown in Fig. 2 of the main text.

We again start from an initial state of the form in Eq. 13 where we take ρ_S to be the maximally mixed state and $|v_j\rangle$ to be the eigenstate of Y_j with eigenvalue $+1$. However, given the ergodic nature of the FMFIC, the choice of the state $|v_j\rangle$ is immaterial. The results for $\Delta_k(t)$ are shown in Fig. S4. The behaviour of $\Delta_k(t)$ as a function of time t and system size L is qualitatively indistinguishable from that of the KIC, thus demonstrating the general robustness of our results.

VIII. MODELS WITH WEAK ERGODICITY BREAKING: PXP MODEL

Throughout this work, our motivation has been to understand the physics of mixed-state deep thermalisation under chaotic/ergodic unitary dynamics. On the other hand, the question of the fate of mixed-state deep thermalisation in the case of ergodicity broken systems is certainly an important and interesting extension of this. A comprehensive exploration of this topic lies beyond the scope of the present work. However, as proof of principle we present some preliminary numerical results in this section for a model with weak ergodicity breaking.

Specifically, we consider a version of the PXP model, described by the Hamiltonian

$$H = H_{\text{PXP}} + H_\mu = \sum_j P_{j-1} X_j P_{j+1} + \mu \sum_j Z_j, \quad P_j = (1 - Z_j)/2, \quad (\text{S54})$$

which is an archetypal model for weak ergodicity breaking via quantum many-body scars. For this model, Ref. [31] found that while all initial states ultimately deeply thermalise, scarring states exhibit significantly longer deep-thermalisation timescales.

To adapt this setting to our mixed-state framework, we considered initial states of the form Eq. 13 (in the main text), with $\rho_S \propto \mathbb{I}_{D_S}$ and the pure-state component $\prod_{j \in E} |v_j\rangle\langle v_j|$ chosen to be either a scarring state ($|Z_2\rangle$) or a non-scarring state ($|Z_4\rangle$). Here $|Z_2\rangle = |\uparrow\downarrow\uparrow\downarrow \cdots \uparrow\downarrow\rangle$ and $|Z_4\rangle = |\uparrow\downarrow\downarrow\uparrow\uparrow\downarrow\downarrow \cdots \uparrow\downarrow\downarrow\rangle$.

We then examined the dynamics of the deep-thermalisation measure $\Delta_k(t)$. The results are shown in Fig. S5 for different values of $|S|$.

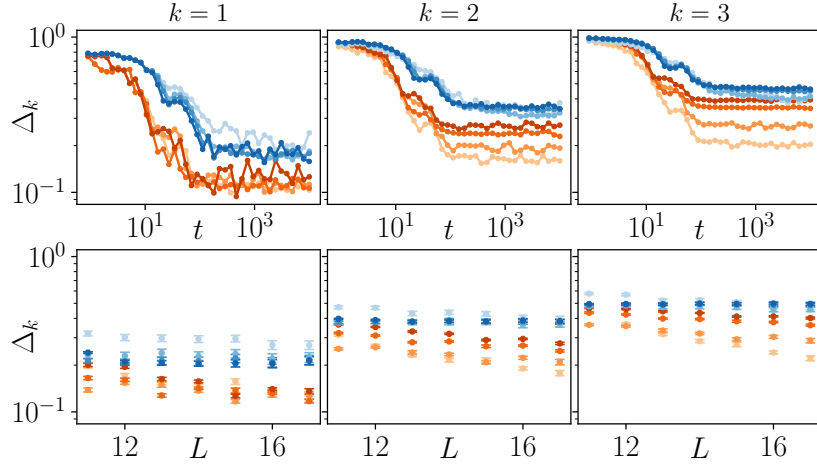


FIG. S5. Results for $\Delta_k(t)$ for the PXP model defined in Eq. S54 with $|A| = 3$ and $\mu = 0.05$. The initial state is of the form in Eq. 13 of the main text, with S in a maximally mixed state and E either $|Z_2\rangle$ (blue) or $|Z_4\rangle$ (red). Different intensities correspond to subsystem sizes $|S| = 0, 2, 4, 6$ (tuning the mixedness), with darker colours denoting larger $|S|$. Upper panels: time evolution of $\Delta_k(t)$ for total system size $L = 17$. Lower panels: long-time average as a function of L .

The results show that the overall phenomenology is robust upon introducing mixed states: the scarring state takes significantly longer to deep-thermalise than the non-scarring one, confirming that the mixed-state version remains a sensitive probe of weak ergodicity breaking. At the same time, increasing the rank of the mixed part of the initial state systematically enhances the deep-thermalisation timescale. This behaviour arises because a mixed initial state explores a larger portion of Hilbert space, thereby sampling more extensively from the family of scarred eigenstates. These effects are most pronounced for $k \geq 2$ and become more marked with increasing k .

Hence, our results can be interpreted in two complementary ways. First, mixed-state deep thermalisation continues to clearly distinguish between scarring and non-scarring initial states, particularly at low rank of the initial mixed state. Second, increasing the mixedness of the initial state amplifies sensitivity to weak ergodicity breaking across the spectrum—potentially providing a practical diagnostic tool for detecting hidden scarring in other models.